Wave-vortex mode coupling in neutrally stable baroclinic flows

Abdelaziz Salhi[1,2] and Alexandre B. Pieri[3,*]

[1]*Département de Physique, Faculté des sciences de Tunis, 1060 Tunis, Tunisia*

[2]*Institute for Advanced Study (IMéRA fellow), Université Aix-Marseille, 2 Place Le Verrier 13004 Marseille, France*

[3]*Institute of the Atmospheric Sciences and Climate, Corso Fiume 4, 10133 Turin, Italy*

(Received 20 January 2014; revised manuscript received 30 May 2014; published 7 October 2014)

Rotating stratified flows in thermal wind balance are at the center of geophysical fluid dynamics. Recently, endeavors were put on studying the linear response of such flows to potential vorticity perturbations. It has been shown that the initial potential vorticity (PV) distribution is fundamental and is responsible for important transient growth of the perturbation and gravity-wave generation. Using Pfeiffer's theorem [J. Differ. Equat. **11**, 145 (1972)], we give the mathematical demonstration of the stability of asymmetric perturbations $k_1 \neq 0$ of a uniform, unbounded flow in thermal wind balance. Incidentally, we prove that both the wave mode (that corresponds to a vanishing PV) and the vortex mode (corresponding to a nonzero PV) are stable. The emphasis is put on the nontrivial behavior of inertia-gravity waves (IGWs) when deformed by a background shear. In particular, we show that in the linear limit, sheared inertia-gravity waves asymptotically oscillate at the inertial waves frequency, but their amplitude is sensitive to shear, stratification, and rotation. Last, we study the development of the IGWs dynamics considering isotropic initial conditions. Computations indicate that both the vortex mode and the wave mode generate IGWs, but the energy of the IGWs generated by the vortex mode is more important than the energy of the IGWs generated by the wave mode. It is also found that, at large times, the energy of the IGWs generated by the vortex mode increases as the ratio k_v/k_h (initial vertical wavenumber over horizontal wavenumber) increases (like k_v^2/k_h^2), while the energy of the IGWs generated by the wave mode oscillates in function of k_v/k_h.

DOI: 10.1103/PhysRevE.90.043003 PACS number(s): 47.32.−y, 47.27.−i, 02.30.Hq, 47.35.Bb

I. INTRODUCTION

Stability analysis of vertically sheared flows in rotating stratified fluids has provided understanding of the large-scale instabilities of the westerly winds in midlatitudes of the atmosphere (e.g., see Refs. [1–3]). Because of its simplicity, the Eady flow [4] has been used in several studies on baroclinic instability. It consists of a parallel flow with uniform vertical shear (with rate Λ) in the presence of a uniform vertical buoyancy gradient (with strength N_v^2) and constant Coriolis frequency f. Under the Boussinesq approximation, thermal wind adjustment [5] imposes a uniform meridional buoyancy gradient $N_h^2 = -\Lambda f$, and

$$\boldsymbol{\nabla} \times \boldsymbol{U} + 2\boldsymbol{\Omega} = (0, \Lambda, f), \quad \Theta = -f\Lambda x_2 + N_v^2 x_3, \quad (1)$$

where $\boldsymbol{U} = (\Lambda x_3, 0, 0)$ and Θ are the basic velocity and buoyancy scalar, respectively.

For a fluid confined between horizontal plates (at $x_3 = 0$ and $x_3 = H$) there are unstable quasigeostrophic (QG) wave solutions [4]. The unstable modes draw their energy from the potential energy of the basic state. The mechanism of energy transfer from the basic shear flow to perturbation mediated by Reynolds stress is not captured by the QG theory that is strictly valid in the limit of a small Rossby number, $\mathrm{Ro} = \Lambda/f$, and a large Richardson number, $\mathrm{Ri} = N_v^2/\Lambda^2$ [6]. The nongeostrophic generalization of the Eady model by Stone [7,8] shows the appearance of linear symmetric instability (independent of the zonal coordinate, x_1) for $\mathrm{Ri} < 1$ (also see Ref. [9]). Symmetric instability causes some physical phenomena in the oceans and the atmosphere (for example, the generation of roll vortices, the origin of rainbands, and squall lines [10,11]). It has also been suggested that this instability is important in the atmospheres of Jupiter, Saturn, and Venus [12,13]. In addition to symmetric instability, another characteristic of the nongeostrophic baroclinic instability problem is the existence of unstable modes beyond the quasigeostrophic Eady cutoff [7]. We recall that in the Eady model, the extent of the horizontal motion must be higher than the Rossby-deformation radius $L_D = N_v D/f$ for baroclinic instability to occur, where D is a vertical length scale. This constraint implies the existence cutoff wavenumber in spectral space, filtering out the smallest scales. This ageostrophic instability can be interpreted as a resonance between boundary mode and inertiagravity mode (e.g., see Refs. [9,14,15]).

The flow Eq. (1) is a linear shear flow (i.e., it presents no inflection point). According to theoretical analysis, linear shear flows are linearly stable for all Reynolds numbers up to infinity (see, e.g., Ref. [16]).

Nonetheless, these flows can exhibit significant *transient growth* for suitable initial perturbations (see, e.g., Ref. [17]).

The transient growth results from the nonnormal character of the operators describing the linear dynamics in linear sheared flows. The corresponding eigenfunctions are nonorthogonal. Hence, when nonlinearities are taken into account modes can strongly interfere for a finite time, limited by phase detuning (see, e.g., Refs. [18–20]). This last mechanism is called *bypass transition* to turbulence and provides a possible solution to the problem of explaining the occurrence of turbulence in otherwise spectrally stable shear flows.

Heifetz and Farrell [6,21] used a generalized stability theory (GST; for details on this energetic method, see Ref. [22]) to analyze the growth of the primitive equations (PE) in response to disturbances of the base flow Eq. (1) in a

*a.pieri@isac.cnr.it

domain that is unbounded horizontally and has planar vertical boundaries. For large Richardson number regime, it is found that the initial PE growth is due to both direct kinetic energy growth mechanism (which is not captured by QG as indicated previously) and interaction between QG modes and gravity waves. For intermediate Richardson number regime, growth rates in the PE greatly exceed those found in the QG analysis only for eddies substantially smaller than the Rossby radius.

Stability analysis of the base flow Eq. (1) under plane wave disturbances with time-dependent wave vector $\boldsymbol{k}$ in an unbounded domain has been addressed by Salhi and Cambon [23]. These advected plane wave disturbances (e.g., see Refs. [24,25]) are often called spatial Fourier harmonics (SFH) [26] and sometimes Kelvin modes (e.g., from Ref. [27]). The stability analysis by Ref. [23] proved that the perturbations with an infinite streamwise wavelength (for which the wavevector becomes time-independent) can exhibit an exponential growth provided that $\mathrm{Ri} < 1$, corresponding to symmetric and baroclinic instability. The effect of the nonlinear interactions on symmetric instability has been recently addressed by Pieri *et al.* [28], who performed direct numerical simulations (DNS) for three-dimensional disturbances of the base flow Eq. (1) considering isotropic initial conditions. In the limit of low Ro, the linear bound for symmetric instability $\mathrm{Ri} = 1$ is recovered.

Time evolution of the linear dynamics of nonsymmetric SFH perturbations that are governed by the following nonhomogeneous second-order differential equations (see Sec. IV C),

$$\ddot{\psi} + \omega^2(t,\boldsymbol{k})\psi = s(t,\boldsymbol{k}), \tag{2}$$

has been recently addressed by Mamatsashvili *et al.* [29] for $\mathrm{Ri} \leqslant 1$. Here, $\psi(t)$ is the amplitude of the SFH mode, and both $\omega(t,\boldsymbol{k})$ and $s(t,\boldsymbol{k})$ are time-dependent functions. For nonsheared rotating gravity waves, the functions $s(t,\boldsymbol{k})$ and $\omega(t,\boldsymbol{k})$ become time-independent. In this case, ω represents the frequency of these dispersive waves. Otherwise, the general solution of the homogeneous equation associated to Eq. (2), i.e., the solution corresponding to a zero value for PV, represents the nongeostrophic IGW mode, while a particular solution of Eq. (2) represents a vortex mode. Mamatsashvili *et al.* [29] have considered an initial state corresponding to a pure vortex mode (wave component set to zero) and observed the generation of IGWs by the vortex mode. Their analysis suggests that the dynamical activity of fronts and jet streaks at $\mathrm{Ri} \leqslant 1$ and $\mathrm{Ro} \geqslant 1$ should be determined by the asymmetric perturbations rather than by the symmetric ones, in agreement with the analysis by Pieri *et al.* [30].

On the other hand, Lott *et al.* [31] investigated the generation of IGWs by three-dimensional PV anomalies considering asymmetric perturbations of the base flow Eq. (1) at hydrostatic equilibrium via a Wentzel-Kramers-Brillouin (WKB) approach. Note that close to PV anomalies, perturbations are in nearly geostrophic balance, whereas beyond the inertia critical levels they have the form of vertically propagating IGWs with amplitudes rapidly decreasing as the Richardson number increases [31]. In the model of Lott *et al.* [31], the wavevector is not time-dependent anymore, and mean shear advection in spectral space is treated as an additional phase. Asymptotic results in terms of the Rossby number Ro are obtained considering a localized quasihorizontal potential vorticity distribution. It is stated that the amplitude of the emitted gravity wave is strongly sensitive to the parameter $\mathrm{Ri}(1+\nu^2)$, where $\nu = k_2/k_1$ is the ratio of the meridional wavenumber to the zonal one. In the present study, we show that this parameter also plays an important role in the dynamics of the nonrotating sheared gravity waves.

The main purpose of the present study is to demonstrate, using Pfeiffer's [32] theorem, that the flow Eq. (1) is neutrally stable under asymmetric disturbances for vertically stable stratification ($\mathrm{Ri} > 0$).

We do not operate on Eq. (2) because the function $\omega^2(t)$ is not impulsively small, meaning that the integral $\int_{t_0}^{\infty} \omega^2(t)dt$ does not converge except for $k_2 = 0$, i.e., an infinite transverse or meridional wavelength. We rather consider the third-order differential equation $\dddot{\psi} + q(t)\dot{\psi} + r(t)\psi = 0$, and we apply Pfeiffer's theorem [32] to demonstrate the stability of the solution.

In addition, we analyze the transient growth of energy for sheared baroclinic flows. We show that after the initial phase, for which there is a transient growth of energy for some orientations of the initial wavevector, the total energy (kinetic + potential) of IGWs behaves like the square of the ratio of the vertical wavenumber to the horizontal one, k_v^2/k_h^2, as in the pure shear flow case. This transient growth is mainly due to the vortex mode.

The paper is organized as follows. First, the mathematical formulation of the problem is given in Sec. II. Second, a brief review on nonrotating sheared gravity waves is presented in Sec. III A. Symmetric instability of sheared rotating stratified flows is then discussed in Sec. III B. The application of Pfeiffer's theorem is presented in Sec. III C to show that the flow Eq. (1) is neutrally stable (intermediate results to check that Pfeiffer's theorem hypothesis are fulfilled are gathered in the Appendix). Wave-vortex mode coupling and its implication on the analysis of the transient growth of energy are then addressed in Sec. IV. Last, Sec. V deals with our concluding remarks.

II. MATHEMATICAL FORMULATION

A. Base flow

We consider a stratified linear shear flow in an unbounded domain rotating uniformly (with rate $\Omega = f/2$) about the vertical axis in the inviscid limit. As in most previous studies on baroclinic instability, we use the Boussinesq approximation, which filters out the higher-frequency acoustic waves. In the Boussinesq approximation, density (or temperature) can fluctuate but the velocity field is assumed to be strictly solenoidal (divergence free). Accordingly, in the inviscid limit, the Euler-Boussinesq equations can be written as follows:

$$\begin{aligned} \boldsymbol{\nabla}\cdot\boldsymbol{U} &= 0, \\ \partial_t \boldsymbol{U} + \boldsymbol{U}\cdot\boldsymbol{\nabla}\boldsymbol{U} &= -\boldsymbol{\nabla}P^* - f\boldsymbol{e}_3\times\boldsymbol{U} + \Theta\boldsymbol{e}_3, \\ \partial_t\Theta + \boldsymbol{U}\cdot\boldsymbol{\nabla}\Theta &= 0, \end{aligned} \tag{3}$$

where

$$P^* = \frac{P}{\varrho_0} - \frac{1}{2}\Omega^2\left(x_1^2 + x_2^2\right),$$

in which P is the pressure, ϱ_0 is a reference density, and (x_1, x_2, x_3) denote the zonal, meridional, and vertical directions, respectively, and where $(\boldsymbol{e}_1, \boldsymbol{e}_2, \boldsymbol{e}_3)$ is the associated canonical orthonormal basis.

The basic velocity field $\boldsymbol{U}$ and buoyancy field Θ under consideration are of the form

$$\boldsymbol{U} = \mathbf{S}\cdot\boldsymbol{x}, \quad S_{ij} = \Lambda\delta_{i1}\delta_{j3}, \quad \Theta = N_h^2 x_2 + N_v^2 x_3, \quad (4)$$

where Λ, N_h, and N_v are constants that represent, respectively, the shear rate and the vertical and horizontal buoyancy frequencies, and δ_{ij} $(i, j = 1, 2, 3)$ is the Kronecker δ. Due to the misalignment of the spanwise basic vorticity vector $\boldsymbol{\nabla}\times\boldsymbol{U} = \Lambda\boldsymbol{e}_2$ with the vertical system rotation $\boldsymbol{\Omega} = (f/2)\boldsymbol{e}_3$, thermal wind adjustment (see, e.g, Ref. [1]) produces a spanwise buoyancy gradient with $N_h^2 = -f\Lambda$ (see Refs. [23,30]). The potential vorticity (see, e.g., Ref. [2]),

$$\Pi = (\boldsymbol{\nabla}\Theta)\cdot(\boldsymbol{\nabla}\times\boldsymbol{U} + 2\boldsymbol{\Omega}) = \left(N_v^2 - \Lambda^2\right)f,$$

constitutes a Lagrangian invariant for the inviscid Boussinesq equations, and its distribution is often relevant to characterize possible flow instabilities (see Refs. [9,33,34]). Conservation of potential vorticity is a direct consequence of Ertel's theorem and can be seen as a generalization of Kelvin's circulation theorem, which applies to barotropic flows (see, e.g., Ref. [2]).

B. The perturbed system

Let $\boldsymbol{U}$, P^*, Θ be replaced by $\boldsymbol{U}+\boldsymbol{u}$, P^*+p, $\Theta+b$ in Eqs. (3) above and linearize. The resulting perturbation equations are

$$\begin{aligned}\partial_t\boldsymbol{u} + \Lambda x_3\partial_{x_1}\boldsymbol{u} &= -\boldsymbol{\nabla}p - \mathbf{S}\cdot\boldsymbol{u} - 2\boldsymbol{\Omega}\times\boldsymbol{u} + b\boldsymbol{e}_3,\\ \partial_t b + \Lambda x_3\partial_{x_1}b &= f\Lambda u_2 - N_v^2 u_3,\end{aligned} \quad (5)$$

with $\boldsymbol{\nabla}\cdot\boldsymbol{u} = 0$. The linearized part of the potential vorticity writes

$$\varpi(\boldsymbol{x},t) = \Lambda\partial_{x_2}b + f\partial_{x_3}b - f\Lambda\omega_2 + N_v^2\omega_3, \quad (6)$$

where $\boldsymbol{\omega} = \boldsymbol{\nabla}\times\boldsymbol{u}$ is the vorticity vector. At any time t, $\varpi(\boldsymbol{x},t)$ is given explicitly in terms of the initial condition $\varpi_0(\boldsymbol{x}) = \varpi(\boldsymbol{x},t=0)$ by (see Ref. [31])

$$\varpi(x_1,x_2,x_3,t) = \varpi_0(x_1 - \Lambda x_3 t, x_2, x_3). \quad (7)$$

Here we search for plane-wave solutions of the form

$$[\boldsymbol{u},p,b,\varpi] = [\hat{\boldsymbol{u}},\hat{p},\hat{b},\hat{\varpi}]\exp[\mathrm{i}\boldsymbol{k}(\tau)\cdot\boldsymbol{x}], \quad (8)$$

where $\boldsymbol{k}$ is the wavevector and $\mathrm{i}^2 = -1$. For a given orientation of the wavevector, the unknowns $[\hat{\boldsymbol{u}},\hat{p},\hat{b},\hat{\varpi}]$ are functions of τ only. The substitution of Eq. (8) into Eq. (5) yields

$$\begin{aligned}&\dot{\hat{\boldsymbol{u}}} + \mathrm{i}[(\dot{\boldsymbol{k}} + \Lambda^{-1}\mathbf{S}^T\cdot\boldsymbol{k})\cdot\boldsymbol{x}]\hat{\boldsymbol{u}}\\ &\quad = \Lambda^{-1}(-\mathrm{i}\hat{p}\boldsymbol{k} - \mathbf{S}\cdot\hat{\boldsymbol{u}} - f\boldsymbol{e}_3\times\hat{\boldsymbol{u}} + \hat{b}\boldsymbol{e}_3),\\ &\dot{\hat{b}} + \mathrm{i}[(\dot{\boldsymbol{k}} + \Lambda^{-1}\mathbf{S}^T\cdot\boldsymbol{k})\cdot\boldsymbol{x}]\hat{b}\\ &\quad = f\hat{u}_2 - \Lambda^{-1}N_v^2\hat{u}_3,\end{aligned} \quad (9)$$

where $\dot{\hat{\boldsymbol{u}}} = d\hat{\boldsymbol{u}}/d\tau$ is the derivative with respect to the dimensionless time $\tau = \Lambda t$ and the exponent T denotes the transpose. The term proportional to $\boldsymbol{x}$ must vanish since the above equations must be valid for any $\|\boldsymbol{x}\|$ due to the fact that the fluid domain is assumed to be unbounded. This is ensuredwhen (see, e.g., Ref. [25])

$$\dot{k}_i = -\Lambda^{-1}S_{ji}k_j. \quad (10)$$

Using the form of S_{ij} given by Eq. (4) and integrating Eq. (10), we obtain

$$k_1 = k_1^0, \quad k_2 = k_2^0, \quad k_3 = k_3^0 - k_1\tau, \quad (11)$$

where $\boldsymbol{k}_0 = (k_1^0,k_2^0,k_3^0)$ is the wavevector at time $\tau = 0$. Therefore, only the vertical component of the wavevector is time-dependent, while the horizontal component remains unaffected by shear. Hereinafter, we denote by $k_h = \sqrt{k_1^2 + k_2^2}$ the horizontal wavenumber, which is time-independent and by $k_v = k_3^0$ the vertical wavenumber at $\tau = 0$. Time dependency of the vertical component $k_3(\tau)$ is induced by the presence of the background shear, but when $k_1 = 0$ (or equivalently, at an infinite streamwise wavelength), k_3 becomes time-independent. Perturbations with $k_1 = 0$ are often called symmetric perturbations in literature (see, e.g., Ref. [35]). Accordingly, the linear differential system, Eq. (9), is rewritten as

$$\begin{aligned}\dot{\hat{\boldsymbol{u}}} &= \Lambda^{-1}(-\mathrm{i}\hat{p}\boldsymbol{k} - \mathbf{S}\cdot\hat{\boldsymbol{u}} - f\boldsymbol{e}_3\times\hat{\boldsymbol{u}} + \hat{b}\boldsymbol{e}_3),\\ \dot{\hat{b}} &= f\hat{u}_2 - \Lambda^{-1}N_v^2\hat{u}_3.\end{aligned} \quad (12)$$

Due to the incompressibility condition, $k_i\hat{u}_i = 0$, we rather consider the following two modes:

$$u^{(1)} = \frac{k_2}{k_h}\hat{u}_1 - \frac{k_1}{k_h}\hat{u}_2 = \mathrm{i}\frac{\hat{\omega}_3}{k_h}, \quad u^{(2)} = -\frac{k}{k_h}\hat{u}_3, \quad (13)$$

instead of $(\hat{u}_1,\hat{u}_2,\hat{u}_3)$. Mode $u^{(1)}$, which is proportional to the vertical vorticity mode $\hat{\omega}_3$, is called toroidal mode, while mode $u^{(2)}$, which is proportional to vertical velocity $\hat{u}_3$, is called poloidal mode. As shown in the Appendix, we deduce from Eq. (12) the following differential system for the toroidal and poloidal modes and the normalized buoyancy mode $u^{(3)} = -(\Lambda/N_v^2)\hat{b}$,

$$\begin{aligned}\dot{u}^{(1)} &= \mathrm{Ro}^{-1}\left(\mathrm{Ro}\frac{k_2}{k} + \frac{k_3}{k}\right)u^{(2)},\\ \dot{u}^{(2)} &= -\mathrm{Ro}^{-1}\frac{k_3}{k}u^{(1)} + \frac{k_1k_3}{k^2}u^{(2)} + \mathrm{Ri}\frac{k_h}{k}u^{(3)},\\ \dot{u}^{(3)} &= \mathrm{Ro}^{-1}\mathrm{Ri}^{-1}\frac{k_1}{k_h}u^{(1)} - \left(\frac{k_h}{k} + \mathrm{Ro}^{-1}\mathrm{Ri}^{-1}\frac{k_2k_3}{k_hk}\right)u^{(2)},\end{aligned} \quad (14)$$

where

$$\mathrm{Ri} = \frac{N_v^2}{\Lambda^2}, \quad \mathrm{Ro} = \frac{\Lambda}{f} \quad (15)$$

are the Richardson number and the Rossby number, respectively. The linearized part of PV, which is a Lagrangian invariant for an inviscid and nondiffusive fluid as indicated previously, can be expressed in terms of the modes $(u^{(1)}, u^{(2)}, u^{(3)})$, as follows

$$\begin{aligned}u_0^{\varpi} &\equiv \frac{\mathrm{i}\hat{\varpi}}{\Lambda f k_0} = \mathrm{RiRo}\frac{k}{k_0}\,c_{12}u^{(3)} + \frac{k}{k_0}c_{32}u^{(1)} + \frac{k_1k}{k_hk_0}u^{(2)},\\ c_{12}(\tau) &= \mathrm{Ro}^{-1}\left(\mathrm{Ro}\frac{k_2}{k} + \frac{k_3}{k}\right),\\ c_{32}(\tau) &= \frac{k_2k_3}{k_hk} + \mathrm{RiRo}\frac{k_h}{k}.\end{aligned} \quad (16)$$

System Eq. (16) will be used in Sec. IV C to study vortex-wave coupling.

III. STABILITY ANALYSIS

In relation with recent studies on baroclinic sheared flows [29,31] we revisit both the case of nonrotating sheared gravity waves and the symmetric instability before demonstrating that the system Eq. (14) is neutrally stable.

A. Nonrotating sheared gravity waves

We briefly review the case of nonrotating sheared gravity waves in an unbounded domain and we attempt to show the role of the parameter $\mathrm{Ri}(1+k_2^2/k_1^2)$ in characterizing the linear dynamics of the gravity waves with or without background rotation. By setting $\mathrm{Ro}^{-1}=0$ and $\xi=\mathrm{i}(k_v-k_1\tau)/k_h$, we deduce from system Eq. (14) the following differential equations for the buoyancy mode $u^{(3)}$ and the vertical velocity mode $\hat{u}_3=-(k_h/k)u^{(2)}$,

$$\frac{d}{d\xi}\left[(1-\xi^2)\frac{du^{(3)}}{d\xi}\right]-\mathrm{Ri}\frac{k_h^2}{k_1^2}u^{(3)}=0,\qquad \frac{du^{(3)}}{d\xi}-\mathrm{i}\frac{k_h}{k_1}\hat{u}_3=0, \tag{17}$$

with solution (see Refs. [36–38])

$$u^{(3)}(\xi)=A_0P_\mu(\xi)+A_1Q_\mu(\xi),\qquad \hat{u}_3(\xi)=-\frac{k_h}{k}u^{(2)}(\xi)=\mathrm{i}\frac{k_1}{k_h}[A_0P'_\mu(\xi)+A_1Q'_\mu(\xi)], \tag{18}$$

where the functions $P_\mu(\xi)$ and $Q_\mu(\xi)$ are Legendre functions of the first and second kind, respectively, and the order μ

$$\mu=\begin{cases}\mu_r=\frac{1}{2}\left(-1+\sqrt{1-4\mathrm{Ri}\frac{k_h^2}{k_1^2}}\right) & \text{if} \quad \mathrm{Ri}<\frac{1}{4}\frac{k_1^2}{k_h^2},\\ \mu_\ell=-\frac{1}{2} & \text{if} \quad \mathrm{Ri}=\frac{1}{4}\frac{k_1^2}{k_h^2},\\ \mu_c=\frac{1}{2}\left(-1+\mathrm{i}\sqrt{4\mathrm{Ri}\frac{k_h^2}{k_1^2}-1}\right) & \text{if} \quad \mathrm{Ri}>\frac{1}{4}\frac{k_1^2}{k_h^2},\end{cases} \tag{19}$$

is the one of the two roots ($\mu=\mu_+$ or $\mu=\mu_-$) of the algebraic equation $\mu(1+\mu)=-\mathrm{Ri}k_h^2/k_1^2$, since $\mu_-+\mu_+=-1$ and $Q_{\mu_-}=P_{-1-\mu_-}=P_{\mu_+}$, $Q_{\mu_+}=P_{-1-\mu_+}=P_{\mu_-}$. Due to the relation

$$P_\mu(\xi)Q'_\mu(\xi)-Q_\mu(\xi)P'_\mu(\xi)=(1-\xi^2)^{-1},$$

we can express the constants A_0 and A_1 in function of the initial values $u_0^{(3)}=u^{(3)}(0)$ and $\hat{u}_{30}=\hat{u}_3(0)$,

$$A_0=\frac{k_h^2}{k_0^2}\left[-\mathrm{i}\frac{k_h}{k_1}Q_\mu(\xi_0)\hat{u}_{30}+Q'_\mu(\xi_0)u_0^{(3)}\right],\qquad A_1=\frac{k_h^2}{k_0^2}\left[\mathrm{i}\frac{k_h}{k_1}P_\mu(\xi_0)\hat{u}_{30}-P'_\mu(\xi_0)u_0^{(3)}\right],\qquad \xi_0=\mathrm{i}\frac{k_v}{k_h}, \tag{20}$$

where the prime denotes differentiation with respect to ξ. For $|\xi|\gg 1$, the functions $P_\mu(\xi)$ and $Q_\mu(\xi)$ behave as (see Ref. [39])

$$P_\mu(\xi)=\frac{2^\mu\Gamma\left(\mu+\frac{1}{2}\right)}{\sqrt{\pi}\Gamma(\mu+1)}\xi^\mu+\frac{\Gamma\left(-\mu-\frac{1}{2}\right)}{2^{\mu+1}\sqrt{\pi}\Gamma(-\mu)}\xi^{-\mu-1},\qquad Q_\mu(\xi)=\frac{\sqrt{\pi}\Gamma(\mu+1)}{2^{\mu+1}\Gamma\left(\mu+\frac{3}{2}\right)}\xi^{-\mu-1}, \tag{21}$$

where $\Gamma(\xi)$ is the γ function, $|\arg(\xi)|<\pi$, and $2\mu\neq\pm1,\pm3,\pm5,\ldots$ Therefore, at large times the modes for which

$$0<\mathrm{Ri}<\frac{1}{4}\frac{k_1^2}{k_h^2},\quad -\frac{1}{2}<\mu=\mu_r<0$$

undergo a power law decay, while the modes for which

$$\mathrm{Ri}>\frac{1}{4}\frac{k_1^2}{k_h^2},\quad \mu=\mu_c=\frac{1}{2}\left[-1+\mathrm{i}\sqrt{4\mathrm{Ri}\frac{k_h^2}{k_1^2}-1}\right]$$

exhibit a damped oscillatory behavior (see Refs. [36,38]). It appears that the parameter $[\mathrm{Ri}(k_h^2/k_1^2)]$ plays an important role in characterizing at least the linear dynamics of the sheared gravity waves even with background rotation (see also Sec. IV A). In fact, as mentioned in the Introduction, Lott *et al.* [31] studied the stability of a homogeneous baroclinic flow submitted to nonsymmetric perturbations at hydrostatic equilibrium. In that study, the perturbed field is expanded in (singular) normal modes parameterized by the phase speed Λx_3,

$$u_3(\boldsymbol{x},t)=\frac{k_1\Lambda}{f}\iiint_{-\infty}^{+\infty}\hat{u}_{30}(k_1,k_2,x_3')\exp\times\mathrm{i}(k_1x_1+k_2x_2-k_1\Lambda x_3't)W(\xi_c)dz'dk_1dk_2, \tag{22}$$

where $W(\xi_c)$ is the structure function of the variable $\xi_c=(k_1\Lambda/f)(x_3-x_3')$ associated to the mode $\hat{u}_3$. It is found that

$$W(\xi)\sim E\xi_c^{1+\mu_c}\quad \text{as}\quad \xi_c\to\infty.$$

At large Ri, we have

$$|\mu_c|\approx\sqrt{\mathrm{Ri}(1+\nu^2)},\quad \nu=k_2/k_1,$$

and according to the WKB approximation, the amplitude E takes the form

$$|E|\sim\frac{\exp(-\nu\pi/2)}{2|\mu_c|^2}\exp(-|\mu_c|\pi/2),$$

signifying that the amplitude of the emitted IGWs is higher for negative values of $\nu=k_2/k_1$. The link between the analysis by Lott *et al.* [31] and the present one, which uses a decomposition of the perturbed field in terms of Fourier modes with time-dependent wavevector, is outside the scope of the present study, which rather focuses on demonstrating the stability of a baroclinic flow under asymmetric disturbances and in analyzing the transient growth of total energy. This topic is addressed in Secs. III C and IV.

B. Case of an infinite streamwise—zonal—wavelength

As indicated in the introduction, Mamatsashvili *et al.* [29] have shown that the transient amplification of nonsymmetric perturbations prevails over symmetric instability (see also Pieri *et al.* [30]). We briefly analyze the evolution of the

dynamics of system Eq. (14) at an infinite streamwise (or zonal) wavelength for which symmetric instability can occur. At $k_1 = 0$, the wavevector becomes time-independent and one easily derives from system Eq. (14) the following dispersion relation:

$$\omega_0^2\Lambda^2 = \underbrace{\left(f^2\sin^2\alpha + N_v^2\cos^2\alpha\right)}_{(I)} + \underbrace{(2\Lambda f\,\sin\alpha\cos\alpha)}_{(II)}, \quad (23)$$

where $\alpha = \arctan(k_v/k_2)$. When $\mathrm{Ri} > 1$, there are sheared inertia-gravity waves,

$$u^{(2)} = u_0^{(2)}\cos(\omega_0\tau) + \left(u_0^{(3)}\mathrm{Ri}\cos\alpha - u_0^{(1)}\mathrm{Ro}^{-1}\sin\alpha\right) \times \frac{\sin(\omega_0\tau)}{\omega_0}, \quad (24)$$

with frequency $\omega_0\Lambda$, propagating in the (x_2, x_3) plane. The term (I) in the latter relation represents the square of the frequency of inertia-gravity waves in the absence of background shear, while the term (II) characterizes the effect of the simultaneous presence of rotation and shear. Therefore, with respect to inertia-gravity waves, sheared inertia-gravity waves propagate faster if $0 < \alpha < \pi/2$ or propagate slower if $\pi/2 < \alpha < \pi$.

When $0 < \mathrm{Ri} < 1$ and the sign of the term (II) in Eq. (23) is negative and its magnitude exceeds that of the term (II), then the sign of ω_0^2 becomes negative, so that

$$\left(f^2 + N_v^2\right) + \left(f^2 - N_v^2\right)\cos 2\alpha < -2\Lambda f\,\sin 2\alpha,$$

signifying the triggering of a linear instability. This instability is called symmetric instability (e.g., see Ref. [35]). Moreover, from relation Eq. (23) one easily verifies that the maximal growth rate, $\sigma_{\max}$, takes the following form (in ft units, see Refs. [29,35,40,41]),

$$\sigma_{\max}^2 = \frac{1}{2}\left[-(\mathrm{Br}+1) + \sqrt{(\mathrm{Br}+1)^2 + 4\mathrm{Br}\frac{(1-\mathrm{Ri})}{\mathrm{Ri}}}\right], \quad (25)$$

where $\mathrm{Br} = \mathrm{RiRo}^2$ is the Burger number [1]. It should be remarked that one can recover relation Eq. (25) by using the pressureless analysis; i.e., one assumes that the velocity, pressure, and density disturbances are time-dependent, but they do not depend on spatial coordinates; see Eq. (59) in Ref. [42]. In the latter study, it is found that the growth rate γ of the kinetic energy E_c,

$$\begin{aligned}
\gamma &= \frac{1}{E_c}\frac{dE_c}{dt} = -\frac{\Lambda u_1 u_3}{E_c} + \frac{u_3 b}{E_c},\\
E_c &= \frac{1}{2}\iiint_{-\infty}^{+\infty}(u^{(1)}u^{(1)*} + u^{(2)}u^{(2)*})d^3\boldsymbol{k},\\
u_1u_3 &= \iiint_{-\infty}^{+\infty}\left[\frac{k_2}{k}\mathrm{Re}(u^{(1)}u^{(2)*}) + \frac{k_1k_3}{k^2}u^{(2)}u^{(2)*}\right]d^3\boldsymbol{k},\\
u_3b &= \frac{N_v^2}{\Lambda}\iiint_{-\infty}^{+\infty}\frac{k_h}{k}\mathrm{Re}(u^{(2)}u^{(3)*})d^3\boldsymbol{k},
\end{aligned} \quad (26)$$

yielded by the linear spectral theory (LST) follows relation Eq. (25), i.e., $\gamma = 2\sigma_{\max}$, for large times $\tau \gg 1$ and $0 < \mathrm{Ri} < 1$ (see their Fig. 5). Here, $*$ denotes complex conjugate. The term $(-\Lambda u_1 u_3)$ represents the energy production due to the background shear, while the term $(u_3 b)$ corresponds to energy gain or loss due to the vertical buoyancy flux. We recall that the QG framework excludes the mechanism of energy transfer from the background shear to perturbations mediated by the Reynolds number (e.g., see Ref. [6]). Obviously, the nonlinear processes act to saturate the exponential instability growth rate as illustrated by the study of Pieri *et al.* [28], who found that the nonlinear growth rate remains less than the one given by Eq. (25).

C. Stability for asymmetric disturbances

In the study by Pieri *et al.* [30] it was stated without giving an exact demonstration that nonsymmetric perturbations are asymptotically bounded. Moreover, the convergence of the two nonzero eigenvalues of the LST system toward $\{-\mathrm{i}f, \mathrm{i}f\}$ suggested the convergence toward a purely oscillating "wave" state at frequency f. The asymptotic amplitude reached by such nonsymmetric modes was shown to depend on the amount of potential vorticity in the flow. This phenomenon results from a strong wave-vortex coupling in the presence of potential vorticity anomalies. By applying Pfeiffer's theorem to the third-order differential Eq. (27), we provide the mathematical demonstration that nonsymmetric perturbations of the thermal wind are necessarily stable and asymptotically oscillatory, completing the previous study by Ref. [30] with asymptotic results.

In Sec. IV C 1 we explain why we consider the third-order differential Eq. (27) to demonstrate the stability of system Eq. (14) and not the nonhomogeneous second-order differential Eq. (2).

From system Eq. (14), we deduce the following third-order differential equation for $y = ku^{(2)}$,

$$\dddot{y} + q(\tau)\dot{y} + r(\tau)y = 0, \quad (27)$$

with the following definition for the time-dependent coefficients:

$$q(\tau) = \mathrm{Ro}^{-2}\left(\mathrm{Ro}\frac{k_2}{k} + \frac{k_3}{k}\right)^2 + (\mathrm{Ri}-1)\frac{k_h^2}{k^2} + \frac{k_1^2}{k^2}, \quad (28a)$$

$$\begin{aligned}
r(\tau) &= -4\mathrm{Ro}^{-1}\frac{k_1k_2k_h^2}{k^4} - 2(\mathrm{Ro}^{-2}-\mathrm{Ri})\frac{k_1k_3k_h^2}{k^4} - 2\mathrm{Ro}^{-2}\frac{k_1k_3}{k^2},\\
\dot{y} &= -\mathrm{Ro}^{-1}k_3u^{(1)} + \mathrm{Ri}k_hu^{(3)},\\
\ddot{y} &= 2\mathrm{Ro}^{-1}k_1u^{(1)} - \left(2\mathrm{Ro}^{-1}\frac{k_2k_3}{k^2} + \mathrm{Ro}^{-2}\frac{k_3^2}{k^2} + \mathrm{Ri}\frac{k_h^2}{k^2}\right)y.
\end{aligned} \quad (28b)$$

When $\mathrm{Ri} > 1$, the function $q(\tau)$ has a positive sign for any value of τ, while, when $\mathrm{Ri} < 1$, its sign is positive only for $\tau > \max(0, d_0)$, where

$$\begin{aligned}
d_0 &= \max(d_1 - d_2, d_1 + d_2),\\
d_1 &= \frac{k_v}{k_1} + \mathrm{Ro}\frac{k_2}{k_1},\\
d_2 &= \mathrm{Ro}\sqrt{(1-\mathrm{Ri})\frac{k_h^2}{k_1^2} - 1}.
\end{aligned} \quad (29)$$

Both $q(\tau)$ and $r(\tau)$ are continuous in $[a,\infty)$, where $a > \max(0,d_0)$ if $0 < \mathrm{Ri} \leqslant 1$ and $a > \max(0,d_1)$ if $\mathrm{Ri} > 1$.

1. Pfeiffer's theorem

In the framework of oscillation theory, Pfeiffer [32] gives five theorems providing estimates on the asymptotic behavior of the solutions of the third-order differential Eq. (27). In the present paper we make use of what is referred to as

Theorem 8. If

$$\ddot{q}q^{-\frac{3}{2}}, \quad \dot{r}q^{-\frac{3}{2}} \quad \text{and} \quad r^2q^{-\frac{5}{2}} \tag{30}$$

are in $L^1(a,\infty)$ and

$$D(\tau) = \pm(\dot{q} - 2r)/q \tag{31}$$

satisfies condition I (see below), then there are three linearly independent solutions $z_i = [y_i, \dot{y}_i, \ddot{y}_i]$ $(i = 1, 2, 3)$ of Eq. (14) and a $\tau_0 \geqslant a$, such that for $\tau \geqslant \tau_0$

$$\begin{aligned} &\mathbf{T}z_1 q^{-\frac{3}{4}} \exp\left[\int_{\tau_0}^{\tau} \frac{r(s)}{q(s)}ds\right] \to p_1, \\ &\mathbf{T}z_\ell q^{-\frac{3}{4}} \exp\left[-\eta_\ell \int_{\tau_0}^{\tau} \sqrt{q(s)}ds - \frac{1}{2}\int_{\tau_0}^{\tau} \frac{r(s)}{q(s)}ds\right] \to p_\ell, \quad (\ell = 2,3), \end{aligned} \tag{32}$$

as $\tau \to \infty$, where

$$\begin{aligned} &\mathbf{T} = \mathrm{diag}\left(q^{\frac{3}{4}}, q^{\frac{1}{4}}, q^{-\frac{1}{4}}\right), \\ &p_\ell = \left(1, \eta_\ell, -\eta_\ell^2\right), \quad (\ell = 1, 2, 3), \end{aligned} \tag{33}$$

with $\eta_1 = 0$, $\eta_2 = \mathrm{i}$, $\eta_3 = -\mathrm{i}$.

Condition I. The function $D(\tau)$ defined on $[a,\infty)$ satisfies Condition I if for some positive constant C^0 either

$$\begin{aligned} &\text{(i)} \quad \int_a^{\tau} D(s)ds \to \infty \quad \text{as} \quad \tau \to \infty \quad \text{and} \\ &\qquad \int_{\tau_1}^{\tau_2} D(s)ds > -C^0 \text{ for } \tau_2 \geqslant \tau_1 \geqslant a \quad \text{or} \\ &\text{(ii)} \quad \int_{\tau_1}^{\tau_2} D(s)ds < C^0 \quad \text{for} \quad \tau_2 \geqslant \tau_1 \geqslant a. \end{aligned} \tag{34}$$

As shown in Appendix B, the functions $(\ddot{q}q^{-\frac{3}{2}})$, $(\dot{r}q^{-\frac{3}{2}})$, and $(r^2q^{-\frac{5}{2}})$ are in $L^1(a,\infty)$. This corresponds to the first set of hypotheses asked by the above theorem. We also prove in Appendix B that the function $D(\tau)$ satisfies Condition I.

2. Application of Pfeiffer's theorem

According to Pfeiffer's theorem, each z_i $(i = 1, 2, 3)$ obeys the following asymptotic behavior:

$$\begin{aligned} &k(\tau)u_1^{(2)}(\tau)\exp\left[\int_a^{\tau} \frac{r(s)}{q(s)}ds\right] \to 1, \\ &k(\tau)u_2^{(2)}(\tau)\exp\left[-\mathrm{i}\int_a^{\tau} q(s)^{\frac{1}{2}}ds - \frac{1}{2}\int_a^{\tau} \frac{r(s)}{q(s)}ds\right] \to 1, \\ &k(\tau)u_3^{(2)}(\tau)\exp\left[\mathrm{i}\int_a^{\tau} q(s)^{\frac{1}{2}}ds - \frac{1}{2}\int_a^{\tau} \frac{r(s)}{q(s)}ds\right] \to 1, \end{aligned} \tag{35}$$

where we have used the initial change of variables $y_i = ku_i^{(2)}$. To conclude on the stability of the solutions we need bounds on the exponential function involved in the asymptotic limits Eq. (35). The computation of such estimates is reported in Appendix C. The final result characterizing the upper bound is given by inequality Eq. (C8), while the final result characterizing the lower bound is given by inequality Eq. (C12). These bounds can be used to derive a stability result for the solutions of Eq. (27). Indeed, applying the exponential function to inequality Eqs. (C8) and (C12) we finally obtain that for all $\tau > a$,

$$|\mathcal{Q}(\tau)|^{\frac{1}{2}} \lesssim \exp\left[\int_a^{\tau} \frac{r(s)}{2q(s)}ds\right] \lesssim |\mathcal{P}(\tau)|^{\frac{1}{2}}, \tag{36}$$

where the notation $\lesssim$ means lower than the compared expression normalized by a constant. $\mathcal{P}(\tau)$ is a second-order polynomial function defined by Eq. (C4) and $\mathcal{Q}(\tau) = \mathcal{P}(\tau) + 4C_q^0$, where C_q^0 is a constant Appendix B [an estimation of C_q^0 is given by (B3)]. In the same way, we obtain

$$|\mathcal{Q}(\tau)| \lesssim \exp\left[\int_a^{\tau} \frac{r(s)}{q(s)}ds\right] \lesssim |\mathcal{P}(\tau)|. \tag{37}$$

Because $\mathcal{Q}(\tau) = \mathcal{P}(\tau) + 4C_q^0$, we have that for $\tau > a$

$$|\mathcal{P}(\tau)|^{\frac{1}{2}} \lesssim \exp\left[\int_a^{\tau} \frac{r(s)}{2q(s)}ds\right] \lesssim |\mathcal{P}(\tau)|^{\frac{1}{2}}, \tag{38}$$

$$|\mathcal{P}(\tau)| \lesssim \exp\left[\int_a^{\tau} \frac{r(s)}{q(s)}ds\right] \lesssim |\mathcal{P}(\tau)|. \tag{39}$$

It can be inferred from Eqs. (38) and (39) that

$$\begin{aligned} k(\tau)|\mathcal{P}(\tau)|^{-\frac{1}{2}} &\lesssim k(\tau)\exp\left[\int_a^{\tau} -\frac{r(s)}{2q(s)}ds\right] \\ &\lesssim k(\tau)|\mathcal{P}(\tau)|^{-\frac{1}{2}}, \end{aligned} \tag{40}$$

$$k(\tau)|\mathcal{P}(\tau)| \lesssim k(\tau)\exp\left[\int_a^{\tau} \frac{r(s)}{q(s)}ds\right] \lesssim k(\tau)|\mathcal{P}(\tau)|. \tag{41}$$

Since $k(\tau) \propto \tau$ and $\mathcal{P}(\tau) \propto \tau^2$, we have that $u_{2,3}^{(2)}$ are asymptotically bounded and oscillates at frequency $\sqrt{q(\tau)}$ and that $u_1^{(2)} \propto \tau^{-3}$ asymptotically vanishes. Therefore, all the nonsymmetric disturbances of the baroclinic equilibrium are stable and generate inertia-gravity waves that asymptotically degenerate into pure inertial waves. This last feature is due to alignment of the mean shear with the rotation axis. We now complete this result giving further details on the role of the initial potential vorticity distribution.

IV. TRANSIENT GROWTH OF ENERGY

A. General considerations

Although the base flow Eq. (4) is neutrally stable (i.e., there are no exponentially growing solutions) for asymmetric disturbances as demonstrated previously, it can exhibit significant "transient growth" in energy because of the nonnormality of perturbation dynamics due to shear. In the bypass transition to turbulence, which has been developed by the hydrodynamic community for spectrally stable shear flows, perturbations

undergo a transient growth. If they have an initially finite amplitude, they may reach an amplitude that is sufficiently large to allow positive feedback through nonlinear interactions that repopulate the growing disturbances. This mechanism could plausibly sustain turbulence for large enough Reynolds numbers. This concept was adopted for unmagnetized stratified accretion disks, since there is irrefutable observational evidence that Keplerian disks have to be turbulent (e.g., see Refs. [43,44]).

Because atmospheric flows are generally nonnormal, the study of the dynamics of the transient growth has been addressed by several authors (e.g., see Refs. [6,21,29,30,45]). As already noticed, in the study by Mamatsashvili *et al.* [29] for baroclinic shear flows with $\mathrm{Ri} \lesssim 1$ and $\mathrm{Ro} \gtrsim 1$, it is found that (SFH) asymmetric perturbations undergo substantial transient amplification much larger than the growth of symmetric instability (see also Ref. [30]), and the largest transition amplification occurs for negative $\nu = k_1/k_2$.

By setting $\boldsymbol{v} = [u^{(1)}, u^{(2)}, \sqrt{\mathrm{Ri}}u^{(3)}]^T$, the spectral density of total energy can be seen as the scalar product

$$2\mathcal{E}_T(\tau) = \langle \boldsymbol{v}(\tau), \boldsymbol{v}(\tau)\rangle = \langle \boldsymbol{v}(0), \mathbf{g}^A\mathbf{g}\cdot\boldsymbol{v}(0)\rangle,$$

where $\mathbf{g}^A = \mathbf{g}^{T*}$ is the transconjugate matrix of the Green matrix $\mathbf{g}$, such that

$$\boldsymbol{v}(\tau, \boldsymbol{k}/k) = \mathbf{g}(\tau, \boldsymbol{k}/k)\cdot\boldsymbol{v}(0, \boldsymbol{k}_0/k_0),$$

where $g_{ij}(0) = \delta_{ij}$. The maximum energy growth $G(\tau)$ obtainable at time τ over all possible initial conditions $\hat{\boldsymbol{v}}(0)$ is (see, e.g., Ref. [46]),

$$G_{\max}(\tau) = \max_{\boldsymbol{v}(0)} \frac{\langle \boldsymbol{v}(0), \mathbf{g}^A\mathbf{g}\cdot\boldsymbol{v}(0)\rangle}{\langle \boldsymbol{v}(0), \boldsymbol{v}(0)\rangle}.$$

In this study, we rather focus on particular initial conditions corresponding to isotropic initial conditions with zero helicity, zero initial potential energy, and zero initial density fluxes (see Appendix A5 in Ref. [44]),

$$\begin{aligned} &u_0^{(1)*}u_0^{(1)} = u_0^{(2)*}u_0^{(2)} = \mathcal{E}_k(0), \\ &u_0^{(3)*}u_0^{(3)} = 0, \quad u_0^{(i)*}u_0^{(j)} = 0 \ (i \neq j), \end{aligned} \tag{42}$$

with $(i, j = 1,2,3)$, so that $\mathcal{E}_T(0) = \mathcal{E}_k(0)$. This choice would be justified by the fact that the turbulence is initially nearly isotropic in usual laboratory experiments on grid turbulence and in direct numerical simulations (DNS). Under the above initial conditions, $\mathcal{E}_T$ can be expressed in terms of components of the matrix $\mathbf{g}$ as

$$\begin{aligned} G &\equiv \frac{\mathcal{E}_T(\boldsymbol{k},\tau)}{\mathcal{E}_T(\boldsymbol{k}_0,0)} = G_k + G_p, \\ G_k &\equiv \frac{\mathcal{E}_k(\boldsymbol{k},\tau)}{\mathcal{E}_T(\boldsymbol{k}_0,0)} = \frac{1}{2}\sum_{i=1}^{2}\sum_{j=1}^{2}|g_{ij}|^2, \\ G_p &\equiv \frac{\mathcal{E}_p(\boldsymbol{k},\tau)}{\mathcal{E}_T(\boldsymbol{k}_0,0)} = \frac{\mathrm{Ri}}{2}\sum_{j=1}^{2}|g_{3j}|^2, \end{aligned} \tag{43}$$

where G_k, G_p, and G characterize the transient growth of kinetic energy, potential energy, and total (kinetic + potential) energy, respectively.

B. Results and discussion

Computations were used to determine the time evolution of the spectral densities for $0 \leqslant \mathrm{Ri} < 10$. A fourth-order Runge-Kutta scheme with time step $\delta\tau = 10^{-3}$ has been used to perform the numerical integration of the system Eq. (14) for g_{ij} with the initial conditions Eq. (44) for $g_{ij}^{(w)}$ (respectively, $g_{ij}^{(v)}(0) = \delta_{ij} - g_{ij}^{(w)}(0)$; see Ref. [44]),

$$g_{ij}^{(w)}(0) = \begin{pmatrix} \frac{1}{1+\psi_0^2} & -\frac{\psi_0}{1+\psi_0^2} & 0 \\ -\frac{\psi_0}{1+\psi_0^2} & \frac{\psi_0^2}{1+\psi_0^2} & -\psi_1 \\ 0 & 0 & 1 \end{pmatrix}. \tag{44}$$

Accuracy was easily assessed by evaluating both the determinant of $\mathbf{g}$, $\det(\mathbf{g}) = k_0/k$ (see Ref. [38]) and the following relation deduced from Ref. [16]:

$$\begin{aligned} &\mathrm{RiRo}\frac{k_h k}{k_1 k_0}c_{12}g_{3j} + \frac{k_h k}{k_1 k_0}c_{32}g_{1j} + \frac{k}{k_0}g_{2j} \\ &\quad = \psi_1\delta_{3j} + \psi_0\delta_{1j} + \delta_{2j}, \end{aligned} \tag{45}$$

$(j = 1,2,3)$, in almost every case examined. Here,

$$\psi_0 = \frac{k_h}{k_1}c_{32}(0), \quad \psi_1 = \mathrm{RoRi}\frac{k_h}{k_1}c_{12}(0). \tag{46}$$

1. *Pure shear flow*

We now focus on the growth amplification of nonsymmetric disturbances in baroclinic shear flows. Theoretical insights can be gained by examining the case of the pure shear flow $(\mathrm{Ri} = 0, \mathrm{Ro}^{-1} = 0)$ for which the matrix $\mathbf{g}$ is 2×2 and found as (e.g., see Ref. [47])

$$\begin{aligned} &g_{11} = 1, \quad g_{21} = 0, \quad g_{22} = \frac{k_0}{k(\tau)}, \\ &g_{12} = \frac{k_0 k_2}{k_1 k_h}\left[\arctan\left(\frac{k_v}{k_h}\right) + \arctan\left(-\frac{k_v}{k_h} + \frac{k_1}{k_h}\tau\right)\right]. \end{aligned} \tag{47}$$

We note that, when k_v and k_1 have opposite signs, the vertical wavenumber $k_3(\tau)$ is either negative or positive and both g_{12} and g_{22} have a monotonic behavior. In particular, g_{22} decreases with time $[g_{22}(0) = 1]$, approaching zero as $\tau \to \infty$, while $|g_{12}|$ grows with time $[g_{12}(0) = 0]$, approaching the limit

$$\left|\frac{k_0 k_2}{k_1 k_h}\left[\arctan\left(\frac{k_v}{k_h}\right) \pm \frac{\pi}{2}\right]\right|,$$

as $\tau \to \infty$. Hence, the contribution of the horizontal kinetic energy to the eventual growth of the kinetic energy prevails over the contribution of the vertical kinetic energy, since

$$\begin{aligned} \frac{\mathcal{E}_v(\tau)}{\mathcal{E}_k(0)} &\equiv \frac{1}{2}\frac{\hat{u}_3\hat{u}_3^*}{\mathcal{E}_k(0)} = \frac{1}{2}\frac{k_h^2}{k^2}\sum_{j=1}^{2}|g_{2j}|^2 \\ &= \frac{1}{2}\frac{\left(1 + \frac{k_v^2}{k_h^2}\right)}{\left[1 + \left(\frac{k_v}{k_h} - \frac{k_1}{k_h}\tau\right)^2\right]^2} \end{aligned} \tag{48}$$

decays with time.

When $k_1 k_v > 0$, the vertical wavenumber takes a zero value at $\tau_0 \equiv k_v/k_1$. During the initial phase, $0 \leqslant \tau < \tau_0$, the vertical kinetic energy grows with time and reaches a maximum value at $\tau = \tau_0$, $\mathcal{E}_v(\tau_0) = (1 + k_v^2/k_h^2)\mathcal{E}_k(0)/2$.

Accordingly, one may conclude that the transient growth of the vertical kinetic energy due to nonsymmetric disturbances in the pure shear case becomes larger for $|k_v|/k_h \gg 1$. Moreover, for $|k_2/k_1| \ll 1$ and in a neighbourhood of $\tau = \tau_0$, the contribution of the vertical kinetic energy is not dominated by the contribution of the horizontal kinetic energy,

$$\frac{\mathcal{E}_h(\tau)}{\mathcal{E}_k(0)} = \frac{\mathcal{E}_k(\tau)}{\mathcal{E}_k(0)} - \frac{\mathcal{E}_v(\tau)}{\mathcal{E}_k(0)} = \frac{1}{2} + \frac{k_0^2 k_3^2}{2k^4} + \frac{k_0^2 k_2^2}{2k_1^2 k_h^2} \times \left[\arctan\left(\frac{k_v}{k_h}\right) - \arctan\left(\frac{k_3}{k_h}\right)\right]^2. \quad (49)$$

After the initial phase, i.e., $\tau > \tau_0$, the spectral density of the vertical kinetic energy decays with time approaching zero for long times. The long-time behavior of kinetic energy is then mainly due to horizontal motions,

$$\lim_{\tau\to\infty} G_k = \lim_{\tau\to\infty} \frac{\mathcal{E}_k(\tau)}{\mathcal{E}_k(0)} = \nu^2\left(1 + \frac{k_v^2}{k_h^2}\right) \times \left[\arctan\left(\frac{k_v}{k_h}\right) + \frac{\pi}{2}\right]^2. \quad (50)$$

Therefore, at $|k_v|/k_h \gg 1$, the spectral density of kinetic energy behaves like $\mathcal{E}_k = \mathcal{E}_v + \mathcal{E}_h \sim (k_v/k_h)^2$, as illustrated by Fig. 1(a). In the next paragraph, we examine the long-time behavior of the spectral density of total (kinetic + potential) energy in baroclinic shear flows and we show that it also behaves like $\mathcal{E}_T = \mathcal{E}_k + \mathcal{E}_P \sim (k_v/k_h)^2$ for large $|k_v|/k_h$.

2. *Baroclinic shear flow*

For a baroclinic shear flow, the matrix **g** is computed numerically, as already indicated. Computations indicate that, after the initial phase defined by $0 \leqslant \tau < \tau_0 = k_v/k_1$, for which there is a transient amplification, all the elements of the matrix **g** exhibit an oscillatory behavior with large amplitude. The time—in ft units, which is normalizing by the rotation time $1/f$—between two successive maximums (or minimums) is 2π. The amplitude of the oscillations depends on both the Richardson and Rossby numbers and also on the orientation of the initial wavevector $\boldsymbol{k}_0/k_0$. Physically, these oscillations correspond to the generated IGWs (e.g., see Ref. [29]). In the following, we examine the long-time behavior of the IGWs energy for $0 < \mathrm{Ri} \leqslant 10$, and we show that, at sufficiently large k_v/k_h, it behaves like $\mathcal{E}_k \sim (k_v/k_h)^2$, as in the pure shear flow case.

Figure 1(b) shows the time evolution of the spectral density of the kinetic energy normalized by its initial value,

$$G_k = \frac{\mathcal{E}_k(\tau)}{\mathcal{E}_k(0)} = \frac{1}{2}\left(g_{11}^2 + g_{12}^2 + g_{21}^2 + g_{22}^2\right),$$

for $\nu = k_2/k_1 = 0.2$, $k_v/k_1 = 80$, $\mathrm{Ro} = 10$, and $\mathrm{Ri} = 0.3,\ 0.9,\ 1.5,\ 5$. We note that the case with $\mathrm{Ri} = 0.3$ and $\mathrm{Ro} = 10$ may occur for fronts and jets (e.g., see Ref. [48]). As shown by Mamatsashvili *et al.* [29], the maximal dominance of asymmetric disturbances over symmetric exponential instability occurs at $\mathrm{Ri} = 0.9$ and $\mathrm{Ro} = 10$. As it can be seen from Fig. 1, at sufficiently large time, there are no significant

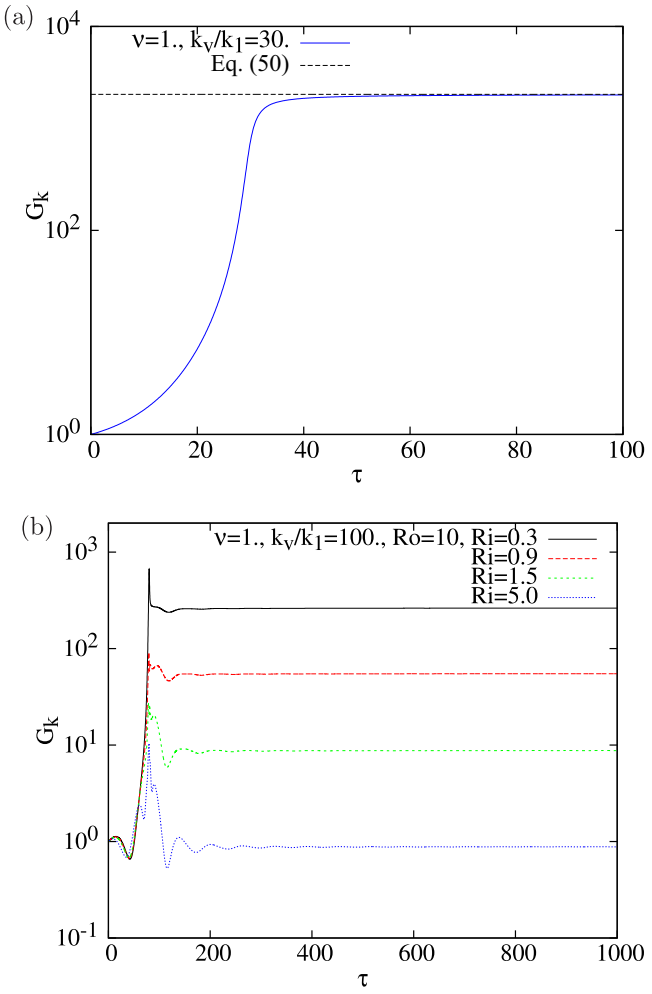

FIG. 1. (Color online) Time evolution of $G_k = \mathcal{E}_k(\tau)/\mathcal{E}_k(0)$ in pure shear flow ($\mathrm{Ri} = 0$, $\mathrm{Ro}^{-1} = 0$, upper panel) and in baroclinic shear flow ($\mathrm{Ro} = 10$ and $\mathrm{Ri} = 0.3,\ 0.9,\ 1.5,\ 5.0$, lower panel) for $\nu = k_2/k_1 = 1$ and $k_v/k_1 = 30$ (a) and $k_v/k_1 = 100$ (b). The figure shows that, at large times, there is no appreciable variation of G_k and the level of energy decreases as Ri increases.

variations for the development of $G_k(\tau)$. This is a consequence of the fact that the trajectory in the two-dimensional phase spaces $\{g_{11}, g_{21}\}$ and $\{g_{12}, g_{22}\}$ has a "circular" shape for long times. Note that when considering the long-time limit of the right-hand side of the two first equations in Eq. (14), we obtain the following system:

$$g_{11}\dot{g}_{11} + g_{21}\dot{g}_{21} = 0,$$
$$g_{12}\dot{g}_{12} + g_{22}\dot{g}_{22} = 0,$$

for which the trajectory, in the two-dimensional phase space $\{g_{1j},\ g_{2j}\}$, is indeed circular. Obviously, the radius of the circular trajectory is intimately tied to the dynamics of system Eq. (14) during the transient phase. The shear would also play an important role since we show that, at sufficiently large k_v/k_h, the growth of the IGWs energy behaves like (k_v^2/k_h^2) for large times.

The variation of G_k at large time ($\tau = 8\tau_0 = 8k_v/k_1$) in function of the ratio k_v/k_h for fixed values of the triplet (Ri, Ro, ν) is shown in Fig. 2. Figures 2(a), 2(b), and

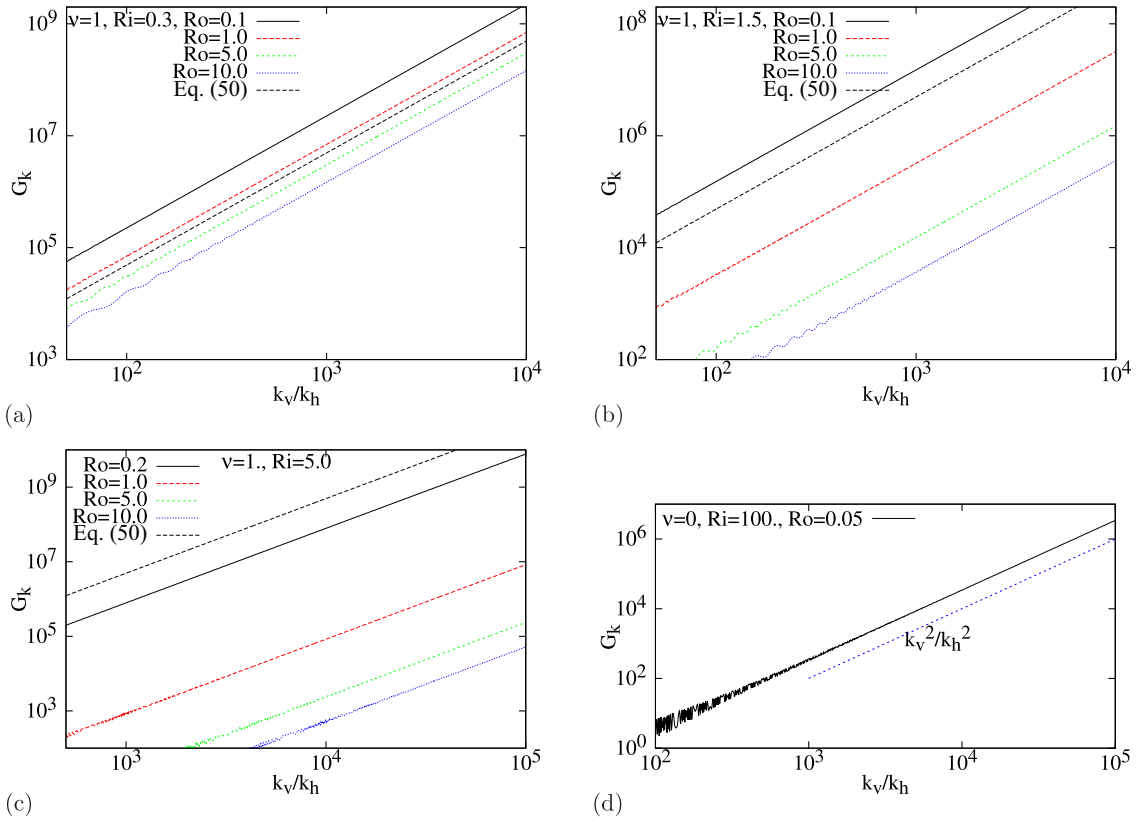

FIG. 2. (Color online) Variation of the long-time limit ($\tau = 8\tau_0 = 8k_v/k_h$) of the IGWs kinetic energy $G_k = \mathcal{E}_k(t)/\mathcal{E}_k(0)$ versus k_v/k_h in baroclinic shear flows. (a) Ri = 0.3, Ro = 0.1, 1.0, 5.0, 10.0, and $k_2/k_1 = 1$. (b) Ri = 1.5, Ro = 0.1, 1.0, 5.0, 10.0, and $k_2/k_1 = 1$. (c) Ri = 5.0, Ro = 0.2, 1.0, 5.0, 10.0, and $k_2/k_1 = 1$. (d) Ri = 100, Ro = 0.05, and $k_2/k_1 = 0$. The figure reveals that, when $k_v/k_h \gg 1$, G_k behaves like k_v^2/k_h^2 as in the pure shear flow.

2(c) display the results obtained for $\nu = k_2/k_1 = 1.0$, Ro = 0.1, 0.2 1.0, 5.0, 10.0, and Ri = 0.3 (a), Ri = 1.5 (b), and Ri = 5.0 (c). As can be expected, at fixed k_v/k_h, the long-time limit of G_k decreases as Ro (or Ri) increases. The present numerical results (performed for Ro $\leqslant$ 10) show that, with respect to the pure shear case, there is an increase of the kinetic energy when shear and rotation are simultaneously present (Ro $\neq 0$ and Ri $= 0$). Stable vertical stratification acts to reduce this increase when shear, rotation, and vertical stratification are simultaneously present. For some values of Ro, Ri, and ν, there is a balance between rotation and vertical stratification on the kinetic energy of the IGWs, so that it approximately follows Eq. (50) for a pure shear flow. This explains the fact that some curves in Fig. 2 are located above the curve associated with Eq. (50). It clearly appears from Figs. 2(a), 2(b), and 2(c) that, at sufficiently large k_v/k_h, the long-time limit of the spectral density of the kinetic energy behaves like $\mathcal{E}_k \propto (k_v/k_h)^2$ as in the pure shear case. Computations indicate that for large Ri($\lesssim$100), G_k also behaves like $(k_v/k_h)^2$, provided $0 <$ RoRi $= N_v^2/(fS) = N_v^2/|N_h^2| \lesssim 5$ and $\nu \leqslant 1$ as illustrated by Fig. 2(d) obtained for Ri = 100, Ro = 0.05, and $k_2 = 0$ (so that $\nu = 0$).

In the two-dimensional phase space $\{g_{31}, g_{32}\}$ the trajectory (for long times) has an elliptical shape and accordingly the spectral density of the potential energy of the IGWs [see the third relation in Eq. (43)] exhibits an oscillatory behavior for long times. Therefore, the spectral density of total energy (kinetic + potential) of the IGWs also exhibits an oscillatory behavior as illustrated by Fig. 3 obtained for Ri = 0.3, Ro = 10, $\nu = 1$, and $k_v/k_h = 100$. For a given value of the quadruplet (Ri, Ro, ν, k_v/k_h) such that $k_v/k_h \gg 1$ and ν is not very large, the total energy of IGWs oscillates about a constant value $\overline{\mathcal{E}}_T$ and the amplitude of these oscillations approximatively equalizes the amplitude of the potential energy $\mathcal{E}_p$; see Fig. 3(a). As for the variation of $\overline{\mathcal{E}}_T$ versus k_v/k_h for sufficiently large k_v/k_h, it behaves like k_v^2/k_h^2, or equivalently, $\overline{\mathcal{E}}_T \propto L_h^2/L_v^2$, where L_h and L_v such that $L_h k_h \sim 1$ and $L_v k_v \sim 1$ are characteristic horizontal and vertical length scales, respectively, as illustrated by Fig. 3(b).

C. Wave-vortex mode coupling

In this section we attempt to show that the important transient growth of the IGWs energy occurring for some orientations of the initial wavevector is mainly due to the vortex mode.

1. The solution associated to the wave mode and the vortex mode is stable

In view of relation Eq. (16), which translates the fact that PV is a Lagrangian invariant, an alternative formulation of system Eq. (14) into an inhomogeneous second-order differential

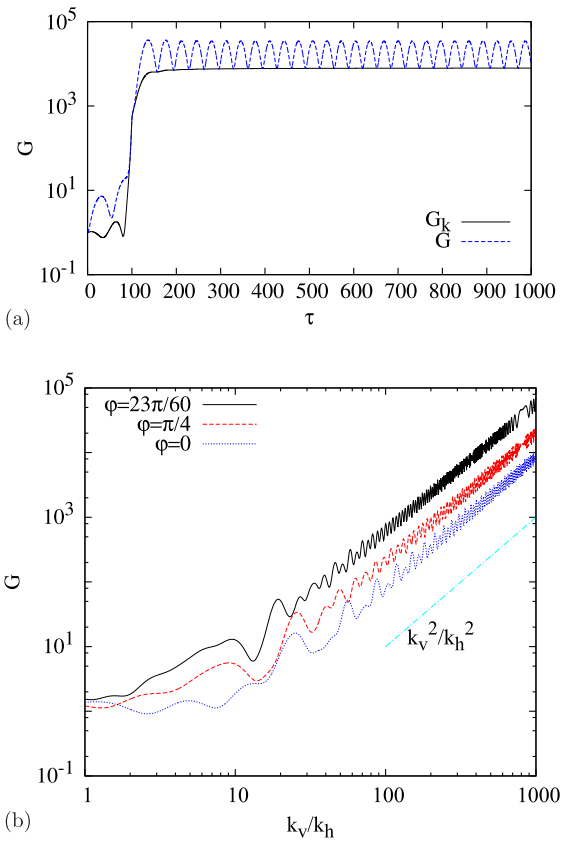

FIG. 3. (Color online) (a) Time evolution of $G = \mathcal{E}_T(t)/\mathcal{E}_T(0)$ in baroclinic shear flow with Ri = 0.3, Ro = 10, $k_v/k_1 = 300$, and $\nu = k_2/k_1 = 1$. At large time, the IGWs kinetic energy is approximately constant, while the total energy (kinetic + potential) oscillates about a constant value $\overline{\mathcal{E}}_T$. (b) Variation of G versus k_v/k_h at large time ($\tau = 2k_v/k_1$) for Ri = 1.5, Ro = 5.0, and three values of $\nu = k_2/k_1 = \arctan(\varphi)$. The figure shows that, at sufficiently large k_v/k_h, there is an important transient growth rate of energy and $\overline{G} = \overline{\mathcal{E}}_T(t)/\mathcal{E}_T(0)$ behaves like k_v^2/k_h^2 as in the pure shear flow case (Ri = 0,$\mathrm{Ro}^{-1} = 0$).

equation yields

$$\ddot{u}^{(1)} + h(\tau)\dot{u}^{(1)} + q(\tau)u^{(1)} = \mathrm{Ro}^{-1}\frac{k_h k_0}{k^2}u_0^{\varpi}, \qquad (51)$$

where

$$h(\tau) = \frac{2k_1}{(k_3 + \mathrm{Ro}k_2)} - \frac{2k_1k_3}{k^2} = \frac{d}{d\tau}\log\left[\left(\mathrm{Ro}\frac{k_2}{k} + \frac{k_3}{k}\right)^{-2}\right], \qquad (52)$$

and $q(\tau)$ is described by Eq. (28a). The functions $h(\tau)$ and $q(\tau)$ are continuous in $[a,\infty)$ and $q''(\tau)/q^{3/2}$ and $h(\tau)$ are in $L^1[a,\infty)$. Therefore, according to corollary 2 (p. 200) in Rovder [49], the homogeneous Eq. (51) has the fundamental system $u^{(1)}_{w\pm}(\tau)$, such that

$$u^{(1)}_{w\pm}(\tau) = q(\tau)^{-\frac{1}{4}}\exp\left[\pm\imath\int_a^\tau q(s)^{\frac{1}{2}}ds\right][1 + o(1)]. \qquad (53)$$

It follows that the particular solution $u_v^{(1)} = u^{(1)} - u_w^{(1)}$ of Eq. (51) is bounded as $\tau \to \infty$ since $u^{(1)}$ is bounded as $\tau \to \infty$, as shown in Sec. III C. The couple $(\boldsymbol{u}_w, \boldsymbol{u}_v)$ characterizes the wave-vortex mode coupling as first shown by Chagelishvili *et al.* [26],

$$u^{(i)}(\boldsymbol{k},\tau) = \underbrace{u_w^{(i)}(\boldsymbol{k},\tau)}_{\text{wave}} + \underbrace{u_v^{(i)}(\boldsymbol{k},t)}_{\text{vortex}}. \qquad (54)$$

Moreover, according to the decomposition Eq. (54), one may write

$$u_w^{(i)}(\tau,\boldsymbol{k}) = g_{ij}^{(w)}(\tau)u^{(j)}(0,\boldsymbol{k}_0), \quad u_v^{(i)}(\tau,\boldsymbol{k}) = g_{ij}^{(v)}(\tau)u^{(j)}(0,\boldsymbol{k}_0),$$

and hence,

$$g_{ij}(\tau) = g_{ij}^{(w)}(\tau) + g_{ij}^{(v)}(\tau), \qquad (55)$$

for any time, where $g_{ij}^{(w)}$ and $g_{ij}^{(v)}$ are the Green functions characterizing the "wave" and "vortex" regimes, respectively, i.e., the regimes respectively corresponding to a zero value or a nonzero value for PV.

The reader could ask why we do not operate directly on Eq. (51) to demonstrate the stability of the complete solution. The response is that the term $h(\tau)$ is not impulsively small (see theorem 6 p. 117 in Ref. [50]) and hence one cannot conclude on the stability of the complete solution even if the term in the right-hand side of Eq. (51) is impulsively small and the solution of the homogeneous equation is bounded. We also remark that an alternative transformation of Eq. (51) yields Eq. (2) or $\ddot{\psi} + \omega^2(\tau)\psi = s(\tau)$, as in the study by Mamatsashvili *et al.* [29], where

$$\omega^2(\tau) = q(\tau) - \tfrac{1}{2}\dot{h}(\tau) - \tfrac{1}{4}h^2(\tau).$$

2. *The energy associated to the wave mode and the vortex mode*

The dynamics of the wave-vortex mode coupling in neutrally stable stratified barotropic or baroclinic shear flows has been studied by some authors [29,30,44,51], as indicated in the introduction.

In view of the decomposition Eq. (54), we introduce the energy $\mathcal{E}_T^{(w)}$ (respectively, $\mathcal{E}_T^{(v)}$) associated to the wave (respectively, vortex) mode by replacing in Eq. (43) g_{ij} by $g_{ij}^{(w)}$ (respectively, $g_{ij}^{(v)}$), and we obtain

$$\mathcal{E}_T(\boldsymbol{k},\tau) = \mathcal{E}_T^{(w)}(\boldsymbol{k},\tau) + \mathcal{E}_T^{(w-v)}(\boldsymbol{k},\tau) + \mathcal{E}_T^{(v)}(\boldsymbol{k},\tau), \qquad (56)$$

where $\mathcal{E}_T^{(w-v)}(\boldsymbol{k},\tau)$ is the mutual energy, i.e., the energy characterizing the interaction between the vortex and wave modes. To compute $G^{(w)} = \mathcal{E}_T^{(w)}(\tau)/\mathcal{E}_T(0)$ [respectively, $G^{(v)} = \mathcal{E}_T^{(v)}(\tau)/\mathcal{E}_T(0)$], which is described by Eq. (43), provided we replace g_{ij} by $g_{ij}^{(w)}$ (respectively, $g_{ij}^{(v)}$), we use the following initial condition for $g_{ij}^{(w)}$ (respectively, $g_{ij}^{(v)}(0) = \delta_{ij} - g_{ij}^{(w)}(0)$; see Ref. [44]),

$$g_{ij}^{(w)}(0) = \begin{pmatrix} \frac{1}{1+\psi_0^2} & -\frac{\psi_0}{1+\psi_0^2} & 0 \\ -\frac{\psi_0}{1+\psi_0^2} & \frac{\psi_0^2}{1+\psi_0^2} & -\psi_1 \\ 0 & 0 & 1 \end{pmatrix}, \qquad (57)$$

which satisfies Eq. (45),

$$\psi_1 g_{3j}^{(w)}(0) + \psi_0 g_{1j}^{(w)}(0) + g_{2j}^{(w)}(0) = 0,$$
$$\psi_1 g_{3j}^{(v)}(0) + \psi_0 g_{1j}^{(v)}(0) + g_{2j}^{(v)}(0) = \psi_1\delta_{3j} + \psi_0\delta_{1j} + \delta_{2j} \neq 0, \qquad (58)$$

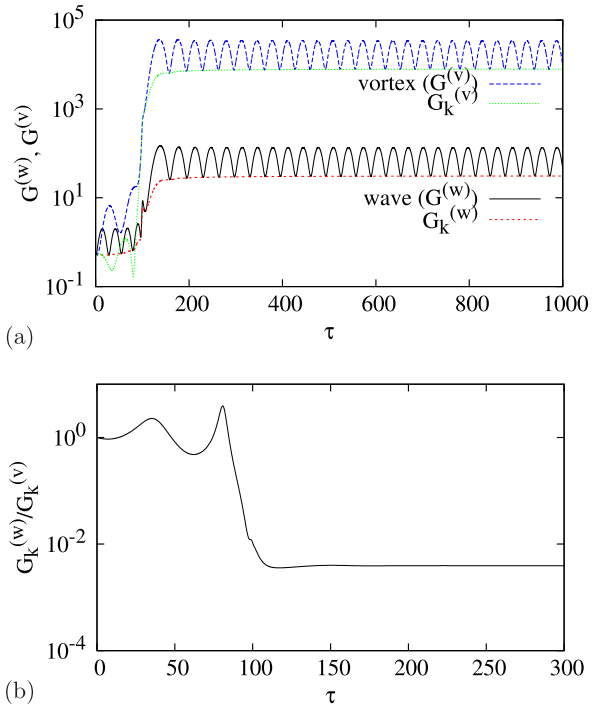

FIG. 4. (Color online) (a) Time evolution of $G^{(v)}$, $G_k^{(v)}$, $G^{(w)}$, and $G_k^{(w)}$ for Ri = 0.3, Ro = 10, $k_v/k_1 = 100.0$, and $\nu = 1$. This panel illustrates the generation of IGWs by the development of both the vortex mode and the wave mode. (b) Time evolution of the ratio $G_k^{(w)}/G_k^{(v)}$ for Ri = 0.3, Ro = 10, $k_v/k_1 = 100.0$, and $\nu = 1$. This panel illustrates that, after the transition period, the energy of the IGWs generated by the vortex mode is more important than the energy of the IGWs generated by the wave mode.

$(j = 1,2,3)$. Therefore, the initial condition for the wave mode is

$$u_w^{(1)}(0) = \frac{1}{1+\psi_0^2}u_0^{(1)} - \frac{\psi_0}{1+\psi_0^2}u_0^{(2)},$$
$$u_w^{(2)}(0) = -\frac{\psi_0}{1+\psi_0^2}u_0^{(1)} + \frac{\psi_0^2}{1+\psi_0^2}u_0^{(2)} - \psi_1 u_0^{(3)}, \qquad (59)$$
$$u_w^{(3)}(0) = u_0^{(3)}.$$

In view of relation Eq. (43), the above initial conditions yield

$$\mathcal{E}_T^{(v)}(0) = \mathcal{E}_T^{(w)}(0) = \tfrac{1}{2}\mathcal{E}_T(0), \quad \mathcal{E}_T^{(v-w)}(0) = 0,$$

signifying that the initial state for which $\mathbf{g}^{(w)}(0) = \mathbf{0}$ mutual energy is initially zero. We note that the initial state for which $g_{ij}^{(v)}(0) = 0$, so that $g_{ij}^{(w)}(0) = g_{ij}(0) = \delta_{ij}$, does not satisfy condition Eq. (58). However, an initial state for which $g_{ij}^{(w)}(0) = 0$, so that $g_{ij}^{(v)}(0) = g_{ij}(0) = \delta_{ij}$, satisfies condition Eq. (58). Consequently, one can consider that the analysis for the development of the growth amplification presented in Sec. IV B corresponds to an initial state for which the initial velocity is a purely vortex mode (i.e., without IGWs). Accordingly, we may conclude that there is a generation of IGWs even if the velocity and density fields are initially a purely vortex mode, in agreement with the analysis of Mamatsashvili *et al.* [29], who considered an initial state corresponding to a pure vortex mode.

Also in the case where the wave mode is not initially zero there is a generation of IGWs by both the vortex mode and the wave mode as illustrated by Fig. 4(a) obtained for Ri = 0.3, Ri = 10, $\nu = 1$, and $k_v/k_1 = 100$. After the transient phase, the energy of the IGWs generated by the vortex mode is more important than the energy of the IGWs generated by the wave mode as illustrated by Fig. 4(b), displaying the time development of $\mathcal{E}_k^{(w)}/\mathcal{E}_k^{(v)}$. An important difference between the IGWs generated by the vortex mode and those generated by the wave mode is that, at asymptotically large times, the energy of the former ones grow with the ratio k_v/k_h [i.e., $\overline{G^{(v)}}$ behaves like (k_v^2/k_h^2)], while the energy of the latter ones oscillates in function of (k_v/k_h) about a constant value as shown by Fig. 5.

V. CONCLUDING REMARKS

Eady's model has been used in several past studies either for a fluid confined between planar vertical boundaries or for a fluid in an unbounded domain. We can consider it as a paradigm to study the dynamics of sheared baroclinic flows occurring in the oceans or in the midlatitude atmosphere. According to the previous stability analysis, there are QG unstable modes, ageostrophic unstable modes (including the symmetric/baroclinic instability), and a generation of IGWs due to potential vorticity anomalies. Because atmospheric

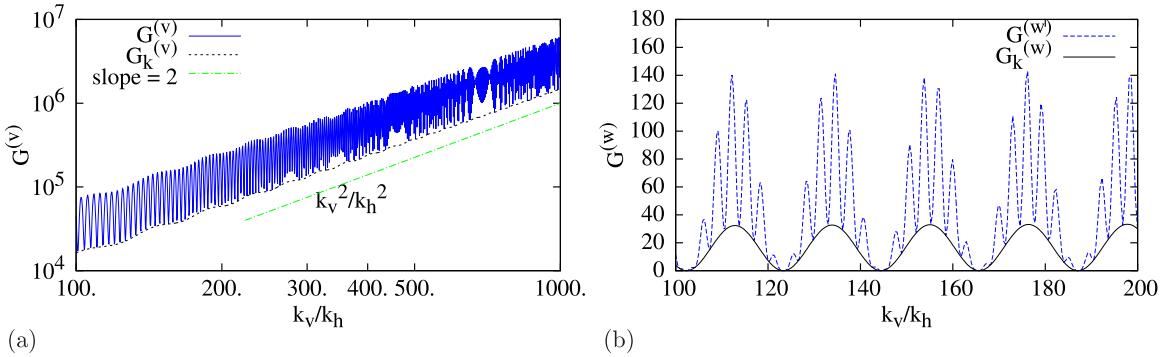

FIG. 5. (Color online) Variation of (a) $G^{(v)}$ and (b) $G^{(w)}$ versus k_v/k_h at large times ($\tau = 8\tau_0 = k_v/k_1$) for Ri = 0.3, Ro = 10, and $\nu = 1$. Panel (a) shows that $G_k^{(v)}$ (the energy of the IGWs generated by the vortex mode) behaves like (k_v^2/k_h^2) for sufficiently large k_v/k_h. Panel (b) shows that $G_k^{(w)}$ (the energy of the IGWs generated by the wave mode) is a periodic function of (k_v/k_h).

flows are generally nonnormal (large scale shear is often present in the atmosphere or in the ocean), the study of the transient dynamics is of capital interest and has been also addressed by some authors. In fact, disturbances may reach an amplitude that is sufficiently large to allow positive feedback through nonlinear interactions that repopulate the growing disturbances. This mechanism could plausibly sustain turbulence for large enough Reynolds numbers.

In the present study, we have considered the Eady like flow described by Eq. (4) in an unbounded domain. Then, we have studied the development of plane-wave disturbances with time-dependent wavevector in the linear limit of an inviscid and nondiffusive Boussinesq fluid. The linear dynamics of the disturbances in the $\boldsymbol{k}$ space is governed by a three-dimensional differential system, $\dot{\boldsymbol{v}} = \mathbf{L}\cdot\boldsymbol{v}$ [see Eq. (12)], where the 3×3 matrix $\mathbf{L}$ is time-dependent and parameterized by the orientation of the wavevector $(\boldsymbol{k}/k)$ and both the Richardson (Ri) and Rossby (Ro) numbers. Using oscillation theory and applying Pfeiffer's theorem [32] to the third-order differential Eq. (27) derived from the system Eq. (12), we have rigorously proved that the flow Eq. (4) is neutrally stable to asymmetric disturbances provided that the vertical stratification is stable ($0 < \mathrm{Ri}$). The analytical developments needed for the proof of this result constitutes an important part of the present study. With the aid of corollary 2 in Rovder [49], this result allows us to prove that the two parts of the solution, i.e., the part corresponding to the wave mode and the part corresponding to the vortex mode, are asymptotically neutrally stable. In fact, the use of PV, which is a Lagrangian invariant for the Euler-Boussinesq equations, allows one to obtain a nonhomogeneous second-order differential equation [see Eq. (2) or Eq. (51)] as an alternative formulation of system Eq. (12). To prove the stability of the solution from this nonhomogeneous second-order differential equation remains a difficult task.

The second part of the present study concerns the characterization of the generated IGWs and the analysis of the transient growth of their energy. As recently shown by Lott *et al.* [31], the IGWs produced by PV anomalies are sensitive to the Richardson number (Ri) and the orientation of the horizontal wave vector ($\nu = k_2/k_1$). The parameter $\nu^2\mathrm{Ri}$ would play an important role, at least, in the linear dynamics of sheared gravity waves with or without rotation as we have shown in Sec. III A.

Due to the nonnormality of linear shear flows, nonsymmetric disturbances (i.e., the disturbances that correspond to a finite streamwise/zonal wavelength $k_1 \neq 0$) can reach an important level of energy at large times. In the pure shear flow case ($\mathrm{Ri} = 0$, $\mathrm{Ro}^{-1} = 0$), we have found that, at large times, the energy of the asymmetric disturbances behaves like k_v^2/k_h^2 [i.e., the square of the ratio of the initial vertical wavenumber to the horizontal one; see Eq. (50)]. Therefore, the amount of energy gained during the transient phase ($0 \leqslant \tau = \Lambda t \leqslant \tau_0 = k_v/k_1$) becomes important for large k_v/k_h (i.e., the initial wavevector is near the vertical axis). For baroclinic shear flows ($0 < \mathrm{Ri}$, $\mathrm{Ro} \neq 0$), the transient phase is also characterized by the amplification period $0 \leqslant \tau \leqslant \tau_0$, as in the pure shear flow case. The IGWs are generated at the beginning of the amplification period and gain energy during this period and eventually maintain it beyond this phase (i.e., at large times; see Ref. [29]). The present numerical results, which were obtained by integrating the system Eq. (12) for several values of the quadruplet $(\mathrm{Ri}, \mathrm{Ro}, \nu, k_v/k_h)$, including the case with $\mathrm{Ri} = 0.3$ and $\mathrm{Ro} = 10$ that can occur in fronts and jets, indicate that, at large times, the level of the IGWs energy is sensitive to shear, stratification, and rotation. In fact, at sufficiently large times, the IGWs energy oscillates with period π (in ft units), but the amplitude of the oscillations is sensitive to shear, stratification, and rotation in addition to the orientation of the initial wavevector. In other words, the amplitude of the oscillations is conditioned by the dynamics of the disturbance during the transient phase. Due to the isotropic initial conditions [see Eq. (42) used in the present paper], it is found that kinetic energy of the IGWs has no appreciable variations at asymptotically large times [see Fig. 1(b)] and for sufficiently large k_v/k_h it behaves like $(k_v/k_h)^2$ as in the pure shear flow (see Fig. 2). The shear signature on the IGWs dynamics would signify that shear plays an important role, and not a minor role. For a fixed value of $(\mathrm{Ri}, \mathrm{Ro}, k_v/k_h, \nu)$ and at large times, the total energy (kinetic + potential) oscillates (with period π in ft units) around a constant value, $\overline{\mathcal{E}}_T$. Also the variation of $\overline{\mathcal{E}}_T$ versus k_v/k_h behaves like $(k_v/k_h)^2$ (see Fig. 3). This behavior of the IGWs energy is mainly due to the vortex mode. In fact, for an initial state at which there is a balance between the energy associated to the wave and the energy associated to the vortex mode, we found that, at large times, the energy of the IGWs generated by the vortex mode is more important to the energy of the IGWs generated by the wave mode (see Fig. 4). In addition, it is found that the energy associated to the vortex mode grows with k_v/k_h (like k_v^2/k_h^2), while the energy associated to the wave mode oscillates with respect to the ratio k_v/k_h (see Fig. 5). Also, it is found that the energy of the IGWs generated by the wave mode is more sensitive to the ratio $\nu = k_2/k_1$ than the energy of the IGWs generated by the vortex mode. Concerning the role the parameter $\nu^2\mathrm{Ri}$ would play in the dynamics of the IGWs, as shown by Lott *et al.* [31], we note that a perturbative method applied to Eq. (51) for sufficiently small Ro^{-1} would allow one to better clarify the role of this parameter. In fact, at $\mathrm{Ro}^{-1} = 0$, Eq. (51) reduces to Eq. (17) which solutions are the Legendre functions $P_\mu(\xi)$ and $Q_\mu(\xi)$, as indicated in Sec. III A. This last aspect will be addressed in a subsequent paper.

ACKNOWLEDGMENTS

Alexandre B. Pieri acknowledges financial support by the Institute of Atmospheric Sciences and Climate (National Research Council, Italy), under Project No. ISAC-005-2012-TO. Aziz Salhi is supported by the Université Aix-Marseille-PIIM laboratory (IMÉRA grant) as a fellow.

APPENDIX A: LINEAR DIFFERENTIAL SYSTEM FOR THE POLOIDAL, TOROIDAL VELOCITY MODES AND THE BUOYANCY MODE

Consider the orthonormal local basis $(\boldsymbol{e}^{(1)}, \boldsymbol{e}^{(2)}, \boldsymbol{e}^{(3)})$ defined by

$$\boldsymbol{e}^{(1)} = \frac{\boldsymbol{k}\times\boldsymbol{e}_3}{\|\boldsymbol{k}\times\boldsymbol{e}_3\|} = \left(\frac{k_2}{k_h}, \frac{-k_1}{k_h}, 0\right),$$
$$\boldsymbol{e}^{(2)} = \frac{\boldsymbol{k}\times\boldsymbol{e}^{(1)}}{k} = \left(\frac{k_1k_3}{k_hk}, \frac{k_2k_3}{k_hk}, \frac{-k_h}{k}\right), \tag{A1}$$

and $\boldsymbol{e}^{(3)} = \boldsymbol{k}/k$, where $k = \|\boldsymbol{k}\|$. In that basis the incompressibility constraint, $\boldsymbol{k}\cdot\hat{\boldsymbol{u}} = 0$, is satisfied by construction, and $\hat{\boldsymbol{u}}$ has only two components: the toroidal mode $u^{(1)} = \hat{\boldsymbol{u}}\cdot\boldsymbol{e}^{(1)}$ and the poloidal mode $u^{(2)} = \hat{\boldsymbol{u}}\cdot\boldsymbol{e}^{(2)}$,

$$u^{(1)} = \frac{k_2}{k_h}\hat{u}_1 - \frac{k_1}{k_h}\hat{u}_2, \quad u^{(2)} = -\frac{k}{k_h}\hat{u}_3.$$

Because the unit vector $\boldsymbol{e}^{(1)}$ is time-independent and the local basis is orthonormal, the equation governing modes $u^{(\alpha)}$ ($\alpha = 1,2$) is simply obtained by projecting the first equation in Eq. (12) on $\boldsymbol{e}^{(\alpha)}$,

$$\dot{u}^{(\alpha)} = -e_1^{(\alpha)}e_3^{(\beta)}u^{(\beta)} + \mathrm{Ro}^{-1}\left[e_1^{(\alpha)}e_2^{(\beta)} - e_2^{(\alpha)}e_1^{(\beta)}\right]u^{(\beta)} + \Lambda^{-1}\hat{b}e_3^{(\alpha)}, \tag{A2}$$

($\alpha, \beta = 1, 2$). Using Eq. (A1) for $e_i^{(\alpha)}$, we express modes $\hat{u}_2$ and $\hat{u}_3$ in the right-hand side of the second equation in system Eq. (12) in terms of modes $u^{(1)}$ and $u^{(2)}$ [see Eq. (13)]. Replacing $\hat{b}$ by $u^{(3)} = -(\Lambda/N_v^2)\hat{b}$, we finally obtain system Eq. (13).

APPENDIX B: APPLICATION OF THE PFEIFFER'S THEOREM

In this appendix, we show that the functions $(\ddot{q}q^{-\frac{3}{2}})$, $(\ddot{r}q^{-\frac{3}{2}})$, and $(rq^{-\frac{5}{2}})$ are in $L^1[a,\infty)$, where $a = \max[0,(\mathrm{Ro}k_2 + k_v)/k_1]$, and the function $D(\tau) = (\dot{q} - 2r)/q$ satisfy Condition I in theorem 8 by Pfeiffer [32].

For the sake of clarity, we report here the expression of the functions $q(\tau)$ and $r(\tau)$ that are given by Eqs. (28a) and (28b), respectively,

$$q(\tau) = \mathrm{Ro}^{-2}\left(\mathrm{Ro}\frac{k_2}{k} + \frac{k_3}{k}\right)^2 + (\mathrm{Ri} - 1)\frac{k_h^2}{k^2} + \frac{k_1^2}{k^2},$$

$$r(\tau) = -4\mathrm{Ro}^{-1}\frac{k_1k_2k_h^2}{k^4} - 2(\mathrm{Ro}^{-2} - \mathrm{Ri})\frac{k_1k_3k_h^2}{k^4} - 2\mathrm{Ro}^{-2}\frac{k_1k_3}{k^2}.$$

We remark that $q(\tau) > 0$ for all dimensionless time $\tau = \Lambda t$ provided that $\mathrm{Ri} > 1$. From the above equations, we state that there exist two positive constants—which depend only on the wavevector $\boldsymbol{k}$—$(C_q^0, C_r^0) \in \mathbb{R}_+^*$ and a time $a > \max[0,(\mathrm{Ro}k_2 + k_v)/k_1]$ (see Sec. IV A), such that $\forall\tau \geqslant a$

$$\left|q(\tau) - \mathrm{Ro}^{-2} + 2\mathrm{Ro}^{-1}\frac{k_2}{k_1}\frac{1}{\tau}\right| \leqslant \frac{C_q^0}{\tau^2}, \tag{B1}$$

$$\left|r(\tau) - 2\mathrm{Ro}^{-2}\frac{1}{\tau}\right| \leqslant \frac{C_r^0}{\tau^2}, \tag{B2}$$

where,

$$C_q^0 \approx \left|-2\mathrm{Ro}^{-1}\frac{k_2k_v}{k_1^2} + \mathrm{Ro}^{-2}\frac{k_v^2}{k_1^2} + \mathrm{Ri}\frac{k_h^2}{k_1^2} - \mathrm{Ro}^{-2}\frac{k_0^2}{k_1^2}\right|,$$

$$C_r^0 \approx 2\mathrm{Ro}^{-2}\left|\frac{k_v}{k_1}\right|,$$

$$\alpha \approx \frac{\mathrm{Ro}}{4}\left(C_q^0 + \frac{k_2^2}{k_1^2}\right)^{-\frac{1}{2}}. \tag{B3}$$

Besides, we have

$$\dot{q}(\tau) = 2\mathrm{Ro}^{-1}\frac{k_1k_2}{k^4}\left(k_3^2 - k_h^2\right) - 2\mathrm{Ro}^{-2}\frac{k_1k_3k_h^2}{k^4} + 2\mathrm{Ri}\frac{k_h^2k_1k_3}{k^4},$$

$$\dot{r}(\tau) = -16\mathrm{Ro}^{-1}\frac{k_1^2k_2k_3k_h^2}{k^6} - 2\mathrm{Ro}^{-2}\frac{k_1^2}{k^4}\left(k_3^2 - k_h^2\right) - 2(\mathrm{Ro}^{-2} - \mathrm{Ri})\frac{k_1^2k_h^2}{k^6}\left(3k_3^2 - k_h^2\right),$$

$$\ddot{q}(\tau) = 2\mathrm{Ro}^{-1}\frac{k_1^2k_2k_3}{k^6}\left(2k_3^2 - 6k_h^2\right) + 2\mathrm{Ri}\frac{k_h^2k_1^2}{k^6}\left(4k_3^2 - k^2\right) - 2\mathrm{Ro}^{-2}\frac{k_1^2k_h^2}{k^6}\left(4k_3^2 - k^2\right), \tag{B4}$$

for the first-order derivative $\dot{q}$, $\dot{r}$ and for the second-order derivative $\ddot{q}$. As a consequence, there exists $a > \max[0,(\mathrm{Ro}\,k_2 + k_v)/k_1]$ (see Sec. IV A), such that $|\ddot{q}q^{-\frac{3}{2}}|$, $|\dot{r}q^{-\frac{3}{2}}|$, and $r^2q^{-\frac{5}{2}}$ are in $L^1(a,\infty)$, which corresponds to the first set of hypothesis asked by *theorem 8* in Pfeiffer [32].

We will now show that Condition I is fulfilled for function $D(\tau)$. From Eqs. (B4) and (28b), we deduce the expression of $(\dot{q} - 2r)$,

$$\dot{q}(\tau) - 2r(\tau) = 2\mathrm{Ro}^{-1}\frac{k_1k_2}{k^2} + 4\mathrm{Ro}^{-1}\frac{k_1k_2k_h^2}{k^4} + 2(3\mathrm{Ro}^{-2} - \mathrm{Ri})\frac{k_1k_3k_h^2}{k^4} + 4\mathrm{Ro}^{-2}\frac{k_1k_3^3}{k^4}. \tag{B5}$$

Since $q(\tau)$ tends to Ro^{-2} as $\tau \to +\infty$, we can focus on the integrability of the numerator of $D(\tau)$. The only nonintegrable term in Eq. (B5) is the last term of the right-hand side, which behaves like τ^{-1} as $\tau \to +\infty$. Therefore, we have

$$\int_a^\tau D(s)ds = 4\mathrm{Ro}^{-2}\int_a^\tau \frac{1}{q(s)}\frac{k_1k_3^3}{k^4}ds + C_D(\tau), \tag{B6}$$

where

$$C_D(\tau) = \int_a^\tau 2\mathrm{Ro}^{-1}\frac{k_1k_2}{k^2} + 4\mathrm{Ro}^{-1}\frac{k_1k_2k_h^2}{k^4} + 2(3\mathrm{Ro}^{-2} - \mathrm{Ri})\frac{k_1k_3k_h^2}{k^4}ds,$$

and

$$\lim_{\tau\to+\infty}\int_a^\tau \frac{1}{q(s)}\frac{|k_1k_3^3|}{k^4}ds = +\infty.$$

We recall that $k_3(\tau) = k_v - k_1\tau$. For $s \gg 1$, we then rewrite the right-hand side of Eq. (B6) as

$$\int_a^\tau D(s)ds = 4\mathrm{Ro}^{-2}\int_a^\tau \frac{1}{q(s)}\frac{(-k_1^4s^3 + O(s^2))}{k^4}ds + C_D(\tau). \tag{B7}$$

The limit of q being positive, the sign of the integral Eq. (B7) is given by $-k_1^4 s^3$ and is then negative. As a consequence,

$$\lim_{\tau\to+\infty}\int_a^\tau +\frac{\dot q(s)-2r(s)}{q(s)} = -\infty,$$

and a natural choice for the constant C^0 is $C^0 = \lim_{\tau\to+\infty}|C_D(\tau)|$. It follows that

$$\lim_{\tau\to+\infty}\int_a^\tau -\frac{\dot q(s)-2r(s)}{q(s)} = +\infty,$$

and

$$-\int_a^\tau \frac{\dot q(s)-2r(s)}{q(s)} > -C^0.$$

APPENDIX C: EVALUATION OF THE UPPER AND LOWER BOUNDS

We first derive bounds on the ratio $r/2q$. From inequality Eqs. (B1) and (B2), we have for all $t > a$

$$\frac{\tau^2}{\mathcal{P}(\tau)+4C_q^0} \leqslant \frac{1}{2q(\tau)} \leqslant \frac{\tau^2}{\mathcal{P}(\tau)}, \tag{C1}$$

and

$$\frac{2\mathrm{Ro}^{-2}\tau - C_r^0}{\tau^2} \leqslant r(\tau) \leqslant \frac{2\mathrm{Ro}^{-2}\tau + C_r^0}{\tau^2}, \tag{C2}$$

leading to

$$\frac{2\mathrm{Ro}^{-2}\tau - C_r^0}{\mathcal{P}(\tau)+4C_q^0} \leqslant \frac{r(\tau)}{2q(\tau)} \leqslant \frac{2\mathrm{Ro}^{-2}\tau + C_r^0}{\mathcal{P}(\tau)}, \tag{C3}$$

where the polynomial $\mathcal{P}$ is defined by

$$\mathcal{P}(\tau) = 2\tau^2\mathrm{Ro}^{-2} - 4\mathrm{Ro}^{-1}\frac{k_2}{k_1}\tau - 2C_q^0. \tag{C4}$$

To this stage, notice that $\Delta = 16\mathrm{Ro}^{-2}(C_q^0 + \frac{k_2^2}{k_1^2})$ is strictly positive.

1. Upper bound

After some factorization we obtain from Eqs. (C3) and (C4):

$$\frac{r(\tau)}{2q(\tau)} \leqslant \frac{1}{2}\frac{\dot{\mathcal{P}}(\tau)}{\mathcal{P}(\tau)} + \left(C_r^0 + 2\mathrm{Ro}^{-1}\frac{k_2}{k_1}\right)\frac{1}{P(\tau)}, \tag{C5}$$

and

$$\frac{1}{2}\frac{\dot{\mathcal{P}}(\tau)}{\mathcal{P}(\tau)+4C_q^0} + \left(-C_r^0 + 2\mathrm{Ro}^{-1}\frac{k_2}{k_1}\right)\frac{1}{\mathcal{P}(\tau)+4C_q^0} \leqslant \frac{r(\tau)}{2q(\tau)}. \tag{C6}$$

The function $\mathcal{P}(\tau)$ admits two real roots (ρ_1,ρ_2), such that

$$\frac{1}{\mathcal{P}(\tau)} = \frac{\alpha}{\tau-\rho_1} - \frac{\alpha}{\tau-\rho_2}, \tag{C7}$$

with $\alpha = \mathrm{Ro}^2(\rho_1-\rho_2)^{-1}/2$. After integration of inequality Eq. (C5) we get upper bound Eq. (C8):

$$\int_a^\tau \frac{r(s)}{2q(s)}ds \leqslant \frac{1}{2}\log\left|\frac{\mathcal{P}(\tau)}{\mathcal{P}(a)}\right| + \left(C_r^0 + 2\mathrm{Ro}^{-1}\frac{k_2}{k_1}\right)\alpha \times \log\left|\frac{\tau-\rho_1}{\tau-\rho_2}\frac{a-\rho_2}{a-\rho_1}\right|. \tag{C8}$$

This is a quite satisfactory upper bound since the log terms will compensate the exponential function in the asymptotic limit Eq. (35).

2. Lower bounds

To conclude on the stability of the solution, we need to find both upper and lower bounds. To obtain a lower bound we must distinguish two cases:

(1) $\mathcal{Q}(\tau) = \mathcal{P}(\tau) + 4C_q^0$ has two distinct real roots or a single root with second-order multiplicity.

(2) $\mathcal{Q}(\tau) = \mathcal{P}(\tau) + 4C_q^0$ has two complex conjugate roots.

a. Case 1

In the first case, if Q has two roots $\rho_1^* \neq \rho_2^*$, we have

$$Q(\tau) = \frac{\alpha^*}{\tau-\rho_1^*} - \frac{\alpha^*}{\tau-\rho_2^*}, \tag{C9}$$

where $\alpha^* = \mathrm{Ro}^2(\rho_1^*-\rho_2^*)^{-1}/2$ and a lower bound is obtained following Eq. (C3). It follows the same calculation presented in the case of the determination of the upper bound. The case of a single root with second-order multiplicity is straightforward.

b. Case 2

In the second case, where Q admits two complex conjugate roots, can be put into the form

$$\mathcal{Q}(\tau) = 2\left(C_q^0 + \frac{k_2^2}{k_1^2}\right)[\Psi^2(\tau)+1], \qquad \Psi(\tau) = \frac{\tau - \mathrm{Ro}\frac{k_2}{k_1}}{\mathrm{Ro}\left(C_q^0 - \frac{k_2^2}{k_1^2}\right)^{1/2}}. \tag{C10}$$

Then, after integration we have

$$\mathfrak{I}(\tau) \equiv \int_a^\tau \frac{ds}{\mathcal{Q}(s)} = \frac{\left(C_q^0 - \frac{k_2^2}{k_1^2}\right)^{-1/2}}{2\mathrm{Ro}^{-1}} \times [\arctan\Psi(\tau) - \arctan\Psi(a)], \tag{C11}$$

and a lower bound is obtained as

$$\frac{1}{2}\log\left|\frac{\mathcal{Q}(\tau)}{\mathcal{Q}(a)}\right| + \left(-C_r^0 + 2\mathrm{Ro}^{-1}\frac{k_2}{k_1}\right)\mathfrak{I}(\tau) \leqslant \int_a^\tau \frac{r(s)}{2q(s)}ds. \tag{C12}$$

From Eq. (C11), we conclude that the integral $\mathfrak{I}(t)$ converges as $\tau \to +\infty$.

[1] P. G. Drazin and W. H. Reid, *Hydrodynamic Stability* (Cambridge University Press, Cambridge, 1981).
[2] J. Pedlosky, *Geophysical Fluid Dynamics* (Springer, New York, 1987).
[3] J. Gula, R. Plougonven, and V. Zeitlin, J. Fluid Mech. **627**, 485 (2009).
[4] E. T. Eady, Tellus **1**, 33 (1949).
[5] G. K. Vallis, *Atmospheric and Oceanic Fluid Dynamics: Fundamentals and Large-scale Circulation* (Cambridge University Press, Cambridge, 2006).
[6] E. Heifetz and B. Farrell, J. Atmos. Sci. **60**, 2083 (2003).
[7] P. H. Stone, J. Atmos. Sci. **23**, 390 (1966).
[8] P. H. Stone, J. Atmos. Sci. **27**, 721 (1970).
[9] M. J. Molemaker, J. C. McWilliams, and I. Yavneh, J. Phys. Oceanogr. **35**, 1505 (2005).
[10] D. B. Parsons and P. V. Hobbs, J. Atmos. Sci. **40**, 2377 (1983).
[11] T. L. Miller and B. N. Antar, J. Atmos. Sci. **43**, 329 (1986).
[12] P. H. Stone, in *Jupiter*, edited by T. Gehrels (University of Arizona Press, Tucson, 1976), pp. 586–618.
[13] G. S. Golitsyn, Icarus **60**, 289 (1984).
[14] N. Nakamura, J. Atmos. Sci. **45**, 3253 (1988).
[15] R. Plougonven, D. J. Muraki, and C. Snyder, J. Atmos. Sci. **62**, 1545 (2005).
[16] B. Mukhopadhyay, N. Afshordi, and R. Narayan, Astrophys. J. **629**, 383 (2005).
[17] P. J. Schmid and D. S. Henningson, *Stability and Transition in Shear Flows* (Springer, Berlin, 2001).
[18] L. Boberg and U. Brosa, Zeitschrift für Naturforschung. A **43**, 697 (1988).
[19] S. C. Reddy, P. J. Schmid, and D. S. Henningson, SIAM J. Appl. Math. **53**, 15 (1993).
[20] S. Grossmann, Rev. Mod. Phys. **72**, 603 (2000).
[21] E. Heifetz and B. Farrell, J. Atmos. Sci. **64**, 4366 (2007).
[22] B. F. Farrell and P. J. Ioannou, J. Atmos. Sci. **53**, 2025 (1996).
[23] A. Salhi and C. Cambon, J. Appl. Mech. **73**, 449 (2006).
[24] Lord Kelvin, Phil. Mag **24**, 188 (1887).
[25] A. D. D. Craik and W. O. Criminale, Proc. R. Soc. London A **406**, 13 (1986).
[26] G. D. Chagelishvili, A. G. Tevzadze, G. Bodo, and S. S. Moiseev, Phys. Rev. Lett. **79**, 3178 (1997).
[27] H. K. Moffatt, in *Atmospheric Turbulence and Radio Wave Propagation* (Nauka, Moscow, 1967), pp. 139–156.
[28] A. B. Pieri, F. S. Godeferd, C. Cambon, and A. Salhi, J. Fluid Mech. **734**, 535 (2013).
[29] G. R. Mamatsashvili, V. S. Avsarkisov, G. D. Chagelishvili, R. G. Chanishvili, and M. V. Kalashnik, J. Atmos. Sci. **67**, 2972 (2010).
[30] A. B. Pieri, C. Cambon, F. S. Godeferd, and A. Salhi, Phys. Fluids **24**, 076603 (2012).
[31] F. Lott, R. Plougonven, and J. Vanneste, J. Atmos. Sci. **69**, 2134 (2012).
[32] G. W. Pfeiffer, J. Differ. Equat. **11**, 145 (1972).
[33] B. J. Hoskins, Q. J. Roy. Meteor. Soc. **100**, 480 (1974).
[34] J. C. McWilliams and I. Yavneh, Phys. Fluids **10**, 2587 (1998).
[35] P. H. Stone, J. Fluid Mech. **45**, 659 (1971).
[36] A. Salhi, Theort. Comput. Fluid Dynam. **15**, 339 (2002).
[37] H. Hanazaki and J. C. R. Hunt, J. Fluid Mech. **507**, 1 (2004).
[38] A. Salhi and C. Cambon, Phys. Rev. E **81**, 026302 (2010).
[39] I. S. Gradshteyn and I. M. Ryzhik, *Table of Integrals, Series, and Products* (Academic Press, New York, 1980).
[40] P. A. Bennetts and B. J. Hoskins, Quart. J. Roy. Meteor. Soc. **105**, 945 (1979).
[41] Q. Xu, Quart. J. Roy. Meteor. Soc. **112**, 315 (1986).
[42] M. Timoumi and A. Salhi, Theort. Comput. Fluid Dynam. **23**, 353 (2009).
[43] A. G. Tevzadze, G. D. Chagelishvili, and J. P. Zahn, Astron. Astrophys. **478**, 9 (2008).
[44] A. Salhi, T. Lehner, F. S. Godeferd, and C. Cambon, Astrophys. J. **771**, 103 (2013).
[45] B. F. Farrell and P. J. Ioannou, J. Atmos. Sci. **66**, 2444 (2009).
[46] H. M. Blackburn, D. Barkley, and S. J. Sherwin, J. Fluid Mech. **603**, 271 (2008).
[47] A. Salhi and C. Cambon, J. Fluid Mech. **347**, 171 (1997).
[48] W. Gu, Q. Xu, and R. Wu, J. Atmos. Sci. **55**, 3148 (1998).
[49] J. Rovder, Arch. Math. (Brno) **22**, 193 (1986).
[50] R. A. Struble, *Nonlinear Differential Equations*, Vol. 267 (McGraw-Hill, New York, 1962).
[51] A. G. Tevzadze, G. D. Chagelishvili, G. Bodo, and P. Rossi, Mon. Not. R. Astron. Soc. **401**, 901 (2010).